

ESTIMATION OF SURFACE ELEVATION CHANGES UNDERNEATH
MANGROVE CANOPY THROUGH GEOSPATIAL AND
GEOMORPHOLOGICAL APPROACH

NORHAFIZI BIN MOHAMAD

UNIVERSITI TEKNOLOGI MALAYSIA

ESTIMATION OF SURFACE ELEVATION CHANGES UNDERNEATH
MANGROVE CANOPY THROUGH GEOSPATIAL AND
GEOMORPHOLOGICAL APPROACH

NORHAFIZI BIN MOHAMAD

A thesis submitted in fulfilment of the
requirements for the award of the degree of
Doctor of Philosophy

Faculty of Built Environment and Surveying
Universiti Teknologi Malaysia

OCTOBER 2022

DEDICATION

This thesis is dedicated to my father, Mohamad Bin Awang, who taught me that the best kind of knowledge to have is that which is learned for its own sake. It is also dedicated to my mother, Siti Mariam Binti Yunus, who taught me that even the most extensive task can be accomplished if it is done one step at a time.

ACKNOWLEDGEMENT

While preparing for this thesis, I was in contact with many individuals, researchers, academicians, and practitioners. Each individual has contributed to helping me understand and practise the knowledge toward successful study in the geoinformatics field. I want to express my infinite appreciation to my main supervisor, Professor Sr. Dr. Anuar Bin Ahmad, for his continuous guidance, support, and precious knowledge in my studies. I am also grateful to cooperate with my co-supervisor, Associate Professor Dr. Ami Hassan bin Md. Din, for his endless advice and motivation. I am incapable of completing this study without the aid of these individuals.

A million thanks to the Ministry of Education (MOE), which provided a previous Trans-Disciplinary Research Grant Scheme (TRGS) Vote No. : RJ130000.7827.4L855, which granted the research opportunity during my master's degree and inspired the idea to expand this research to the doctorate level. This research scheme gives me a perfect kick-start to exploring my journey in the postgraduate world and guides me in a better way to become a researcher in the future.

My gratitude also goes to Universiti Teknologi Malaysia, which funded my doctoral studies through the UTM Zamalah Scholarship. This scholarship scheme boosts my motivation to unleash my true potential in completing my doctorate journey with no financial problems. This scholarship alleviates the financial burden of attending international conferences and seminars, and it also assists me in improving my writing style by providing affordable English editing services.

I also acknowledge the effort of my fellow RA's, other members of TRGS, and my postgraduate friends, who supported me with valuable ideas and technical skills. Some of them who are already experts in this field are very helpful, and I cannot imagine my study progress without their guidance.

Finally, I want to express my gratitude to my entire family, especially my parents, who have blessed my studies and always pray for my success. They also give me motivation to never give up and always focus on completing my studies. Thank you.

ABSTRACT

Estimating surface elevation changes in mangrove forests is dynamic because it is barely visible physically and because of the canopy-covered factor that restricts aerial monitoring. It demands a technique that filters the mangrove canopy at the top of the vegetation and the complex understory structures. Hence, this study estimated surface elevation changes underneath the mangrove canopy through geospatial and geomorphological approaches. The first objective of this study was to discover vegetation filtering algorithms for estimating surface elevation underneath the mangrove canopy, followed by generating an unmanned aerial vehicle-digital elevation model (UAV-DEM) underneath the mangrove canopy with vertical accuracy comparable to physical topography measurement. The other objective was to evaluate the rates of surface elevation changes using the geomorphological change detection method. The last objective was to correlate the interactions between mangrove surface elevation changes and sea level rise. This study's data processing stages included photogrammetric data processing using Structure from Motion-Multiview Stereo (SfM-MVS), filtering using the surface estimation from Nearest Elevation and Repetitive Lowering (SNERL) algorithm, and geomorphological change detection (GCD) analysis. Two epochs of UAV data collection were carried out in 2016 and 2017 at low tide conditions. UAV data processing was performed using the SfM-MVS method. Next, the SNERL algorithm was employed to extract the surface from the mangrove canopy and generate the mangrove ground as a DEM. Subsequently, GCD analysis was utilized to quantify the elevation change rates at the ground surface, which comprise erosion, accretion, and sedimentation, using the differential DEM (DoD) technique. The finding illustrated that the generated UAV-DEM using SNERL algorithms reached vertical accuracy of 0.345 m (RMSE), 0.107 m (mean), and 0.503 m (standard deviation). The other finding indicated that region of interest 5 (ROI 5) experienced the highest volumetric accretion (surface raising) at 0.566 cm³/yr. The highest erosion (surface lowering) was identified at ROI 8 at -2.469 cm³/yr. In contrast, for vertical change average rates, ROI 6 experienced the highest vertical accretion (surface raising) at 1.281 m/yr, while the highest vertical erosion (surface lowering) was spotted at ROI 3 at -0.568 m/yr. In conclusion, a geospatial approach comprising SfM-MVS, vegetation index (VI) segregation, and the SNERL filtering algorithm are efficient in generating UAV-DEM underneath the mangrove canopy at the closest level to the terrain level. The GCD map and the rates of surface elevation changes at Kilim River enabled authorities like Langkawi Development Authority (LADA) and the Department of Drainage and Irrigation (DID) to fully understand the situation and prepare a mitigation plan to avoid unbalanced surface elevation changes that could lead to long-term devastation of the mangrove ecosystem in the future.

ABSTRAK

Menganggarkan perubahan ketinggian permukaan tanah dalam kawasan bakau adalah dinamik kerana ia hampir tidak kelihatan secara fizikal dan kerana teknik litupan kanopi yang menghalang pemantauan udara. Ia memerlukan teknik yang boleh menuras kanopi bakau di bahagian atas tumbuh-tumbuhan dan struktur tanaman rendah yang kompleks. Oleh itu, kajian ini menganggarkan perubahan ketinggian permukaan tanah yang dilitupi kanopi bakau melalui pendekatan geospasial dan geomorfologi. Objektif pertama kajian ini adalah untuk menemui algoritma penurasan tumbuh-tumbuhan untuk menganggarkan permukaan bakau di bawah kanopi bakau, diikuti dengan penjana model ketinggian berdigit-pesawat udara tanpa pemandu (UAV-DEM) di bawah kanopi bakau dengan ketepatan menegak yang setaraf dengan pengukuran topografi secara fizikal. Objektif lain adalah untuk menilai kadar perubahan ketinggian tanah menggunakan kaedah pengesanan perubahan geomorfologi. Objektif terakhir adalah untuk menghubungkan interaksi antara perubahan ketinggian permukaan bakau dengan peningkatan aras laut. Peringkat pemprosesan data dalam kajian ini meliputi pemprosesan data fotogrametrik menggunakan *Structure from motion-multiview stereo* (SfM-MVS), penurasan menggunakan anggaran permukaan dari algoritma ketinggian terdekat dan pengurangan berulang (SNERL) dan analisis pengesanan perubahan geomorfologi (GCD). Dua tempoh masa pengumpulan data UAV telah dijalankan pada 2016 dan 2017 ketika fasa air surut. Pemprosesan data UAV dilakukan menggunakan kaedah SfM-MVS. Seterusnya, algoritma SNERL digunakan untuk mengekstrak permukaan dari kanopi bakau dan menjana permukaan bakau sebagai DEM. Kemudian, analisis GCD telah digunakan untuk mengukur kadar perubahan ketinggian di permukaan tanah, merangkumi hakisan, tokokan dan pemendapan, menggunakan teknik perubahan DEM (DoD). Hasil dapatan menunjukkan bahawa UAV-DEM yang dijana menggunakan algoritma SNERL mencapai ketepatan menegak 0.345 m (RMSE), 0.107 m (min) dan 0.503 m (sisihan piawai). Dapatan lain mendapati bahawa kawasan keutamaan 5 (ROI 5) mengalami tokokan isipadu (kenaikan permukaan) tertinggi pada 0.566 cm³ per tahun. Hakisan isipadu (penurunan permukaan) dikenal pasti pada ROI 8 pada -2.469 cm³ per tahun. Sebaliknya, untuk kadar purata perubahan menegak, ROI 6 mengalami tokokan menegak tertinggi (kenaikan permukaan) pada 1.281 m per tahun manakala hakisan menegak tertinggi (penurunan permukaan) dikesan pada ROI 3 pada -0.568 m per tahun. Sebagai kesimpulan, pendekatan geospasial yang terdiri daripada SfM-MVS, pengasingan indeks tumbuh-tumbuhan (VI) dan algoritma penurasan SNERL adalah berkesan dalam menjana UAV-DEM di bawah kanopi bakau pada ketepatan menghampiri aras permukaan. Peta GCD dan kadar perubahan ketinggian tanah di Sungai Kilim membolehkan pihak berkuasa seperti Perbadanan Pembangunan Langkawi (LADA) dan Jabatan Pengairan dan Saliran (JPS) memahami sepenuhnya keadaan dan menyediakan pelan mitigasi untuk mengelakkan berlakunya ketidakseimbangan perubahan ketinggian tanah yang boleh membawa kepada kemusnahan jangka panjang ekosistem bakau pada masa hadapan.

TABLE OF CONTENTS

	TITLE	PAGE
	DECLARATION	iii
	DEDICATION	iv
	ACKNOWLEDGEMENT	v
	ABSTRACT	vi
	ABSTRAK	vii
	TABLE OF CONTENTS	viii
	LIST OF TABLES	xv
	LIST OF FIGURES	xvii
	LIST OF ABBREVIATIONS	xxii
	LIST OF SYMBOLS	xxvi
	LIST OF APPENDICES	xxviii
CHAPTER 1	INTRODUCTION	1
1.1	Background of Study	1
1.2	Problem Statement	7
1.3	Research Question	10
1.4	Aim and Objectives of Study	11
1.5	Significance of Study	12
	1.5.1 Improving the Existing Filtering Algorithm	12
	1.5.2 Vertical Datum Identification Underneath Mangrove Canopy	13
	1.5.3 Highlighting the Importance and the Contribution of Mangrove	13
1.6	Scope of Study	14
	1.6.1 ‘What’ – Data and Equipment	15
	1.6.2 ‘Where’ – Location of Study Area	15
	1.6.3 ‘When’ – Duration of Study and Date of Data Taken	17
	1.6.4 ‘How’ – Methodology and Technique	17

1.7	General Methodology	18
1.8	Thesis Outline	19
CHAPTER 2	LITERATURE REVIEW	23
2.1	Introduction	23
2.2	Mangrove Ecosystem	23
2.2.1	An Overview of Mangrove Ecosystem	23
2.2.2	Mangrove Surface Topographies and Landform Types	26
2.3	Mangrove Surface Elevation Changes and Its Factor	28
2.3.1	Definition of Mangrove Surface Elevation Changes and Its Process	28
2.3.1.1	Erosion	30
2.3.1.2	Accretion	31
2.3.1.3	Sedimentation	31
2.3.2	Factors of Mangrove Surface Elevation Changes	32
2.3.2.1	Factors of Erosion	32
2.3.2.2	Factors of Accretion	34
2.3.2.3	Factors of Sedimentation	35
2.3.3	Previous Study Related to the Physical Measurement of Surface Elevation Changes	38
2.4	The Interaction Between Mangrove Surface Elevation Changes and Sea Level Rise	41
2.5	An Overview of UAV	45
2.5.1	Introduction to UAV and Its Terminology	45
2.5.2	History and Development Trend in UAV	46
2.5.3	UAV Types, Advantages, and Disadvantages	48
2.5.4	Elements of the Positioning System in UAV Mapping	52
2.6	An Element of Digital Photogrammetry and the SfM-MVS Concept	58
2.6.1	An Overview of Digital Photogrammetry	59
2.6.2	An Overview of SfM-MVS in Digital Photogrammetry	60

2.6.3	The Principle of SfM-MVS	62
2.6.3.1	Feature Detection	63
2.6.3.2	Keypoint Correspondence	64
2.6.3.3	Keypoint Filtering	64
2.6.3.4	Structure From Motion (SfM)	65
2.6.3.5	Scaling and Georeferencing	66
2.6.3.6	Multi-view Stereo (MVS)	67
2.7	Surface Elevation Modelling	68
2.7.1	Digital Surface Model (DSM)	68
2.7.2	Digital Elevation Model (DEM)	69
2.7.3	Digital Terrain Model (DTM)	70
2.8	Vegetation Filtering from UAV-based Photogrammetry Data	71
2.8.1	An Overview of Vegetation Filtering from UAV-based Photogrammetry	71
2.8.2	Previous Study Related to Vegetation Filtering Techniques	73
2.8.3	Vegetation Index (VI) for Segregating Vegetation and Non-Vegetation Areas	76
2.8.4	Surface Estimation Using the Nearest Elevation and Repetitive Lowering Algorithm (SNERL) in a Mangrove Vegetation Area	78
2.9	Quantification of Surface Elevation Changes using Geomorphological Change Detection (GCD) Analysis	81
2.9.1	An Overview of Geomorphological Change Detection (GCD)	81
2.9.2	DEM of Difference (DoD)	82
2.9.3	DEM Error Assessment	83
2.9.3.1	Minimum Level of Detection (minLoD) Threshold	84
2.9.3.2	Map Probabilistic Thresholding using a User-Defined Confidence Interval	85
2.9.3.3	Spatial Variability of Uncertainty from Multiple Parameters	87

2.9.3.4	Spatial Coherence of Erosion and Deposition Units	89
2.9.4	Previous Research on the GCD Quantification Method	89
2.10	Summary of Key Literature Reviews	93
2.10.1	A Critical Review of the Previous Study	93
2.10.2	The Novelty and Contribution of This Study	95
2.11	Chapter Summary	106
CHAPTER 3	METHODOLOGY	107
3.1	Introduction	107
3.2	Methodology	107
3.3	Study Area	110
3.4	Data Collection	111
3.4.1	UAV Data Acquisition	112
3.4.1.1	Specifications of the UAV Model	112
3.4.1.2	UAV Flight Planning	114
3.4.1.3	UAV Data Acquisition	115
3.4.2	GPS Data Acquisition	116
3.4.2.1	Static GPS Surveys for GCP Data Acquisition	116
3.4.2.2	Ground Truth Validation Data Using RTK-GPS Surveys	119
3.4.3	Erosion Pin Data Acquisition	120
3.5	Data Processing	122
3.5.1	SfM-MVS Workflow	123
3.5.1.1	Image Alignment	124
3.5.1.2	Insertion of Ground Control Point (GCP) Data	124
3.5.1.3	Camera and Image Optimisation	125
3.5.1.4	Construction of Point and Dense Cloud Data	125
3.5.1.5	Generating UAV-DSM and Orthophoto	126

3.5.2	Segregation of Vegetation and Non-Vegetation Areas using Vegetation Indices (VI)	126
3.5.3	Vegetation Filtering using the SNERL Algorithm	130
3.5.3.1	Clustering the UAV-DSMs' Height	132
3.5.3.2	UAV-DSM Filtering in the First Iteration	133
3.5.3.3	UAV-DSM Filtering in the Second Iteration	134
3.5.3.4	UAV-DSM Filtering in the Third Iteration	135
3.5.3.5	Final UAV-DEM	136
3.5.4	Quantification of Surface Elevation Changes using the Geomorphological Change Detection (GCD) Method	137
3.6	Data Analysis	139
3.6.1	Accuracy Assessment of GCPs	140
3.6.2	Accuracy Assessment of UAV-DSM (Unfiltered DEM)	141
3.6.3	Accuracy Assessment of UAV-DEM (Filtered DEM)	142
3.6.4	GCD Rate Accuracy Assessment and Erosion Pin	143
3.7	Output of the Study	144
3.8	Chapter Summary	144
CHAPTER 4	RESULTS AND DISCUSSION	145
4.1	Introduction	145
4.2	Result of SfM-MVS Processing	145
4.2.1	UAV Survey Parameters	146
4.2.2	UAV Survey Result	149
4.2.3	Camera Calibration Results	150
4.3	Result of Vegetation Filtering Processing	152
4.3.1	Non-Vegetation Removal Results using Vegetation Index (VI) Filtering	153
4.3.2	SNERL Algorithm Results for Vegetation Filtering	158

4.4	The Result of Geomorphological Change Detection (GCD) Processing	164
4.4.1	Qualitative Analysis of GCD Output	164
4.4.2	Quantitative Analysis of GCD Output	169
4.4.2.1	ROI 1	169
4.4.2.2	ROI 2	170
4.4.2.3	ROI 3	171
4.4.2.4	ROI 4	173
4.4.2.5	ROI 5	174
4.4.2.6	ROI 6	175
4.4.2.7	ROI 7	177
4.4.2.8	ROI 8	178
4.4.3	Summary of GCD Output	188
4.5	Analysis	189
4.5.1	Accuracy Assessment of GCPs	189
4.5.2	Vertical Accuracy Assessment of UAV-DSM (Unfiltered DSM)	191
4.5.3	Accuracy Assessment of the UAV-DEM (Filtered DEM)	193
4.5.4	GCD Rates and Erosion Pin Accuracy Assessment	196
4.6	The Interactions Between Mangrove Surface Elevation Changes and Sea Level Rise	198
4.6.1	Geomorphological Changes Underneath Mangrove Canopy at Kilim River based on Finding	199
4.6.2	Short and Long-Term Impacts of Geomorphological Changes on Mangrove Surfaces and the Interaction with Sea Level Rise	200
4.7	Chapter Summary	201
CHAPTER 5	CONCLUSION AND RECOMMENDATIONS	203
5.1	Fulfilment of Aim, Objectives and Research Questions	203
5.2	Recommendations for Future Studies	207

REFERENCES	211
LIST OF PUBLICATIONS	309

LIST OF TABLES

TABLE NO.	TITLE	PAGE
Table 1.1	Trends in the area of mangroves by region, 1990–2020 (retabulated from FAO, 2020).	4
Table 1.2	The extent of mangroves in Malaysia (retabulated from Omar et al., 2020).	5
Table 2.1	The contribution of surface and subsurface processes to surface elevation change, showing the direction of change (McIvor et al., 2013).	29
Table 2.2	UAV type comparison (Chapman, 2016).	51
Table 2.3	GCP versus UAV-RTK versus UAV-PPK (Blake, 2020).	56
Table 2.4	A chronological list of related previous studies.	98
Table 2.5	The summary of this study.	105
Table 3.1	The specifications of the UAV system used in this study.	114
Table 3.2	UAV flight planning details.	115
Table 3.3	UAV survey data.	116
Table 3.4	Details of GCPs in the study area.	119
Table 4.1	UAV survey data results for all epochs of data collection.	150
Table 4.2	Calibration coefficients and a correlation matrix for all epochs.	152
Table 4.3	Quantitative changes in surface elevation underneath the mangrove canopy at ROI 1.	180
Table 4.4	Quantitative changes in surface elevation underneath the mangrove canopy at ROI 2.	181
Table 4.5	Quantitative changes in surface elevation underneath the mangrove canopy at ROI 3.	182
Table 4.6	Quantitative changes in surface elevation underneath the mangrove canopy at ROI 4.	183
Table 4.7	Quantitative changes in surface elevation underneath the mangrove canopy at ROI 5.	184
Table 4.8	Quantitative changes of surface elevation underneath mangrove canopy at ROI 6.	185

Table 4.9	Quantitative changes in surface elevation underneath the mangrove canopy at ROI 7.	186
Table 4.10	Quantitative changes in surface elevation underneath the mangrove canopy at ROI 8	187
Table 4.11	Geomorphological change detection rates, which show volumetric, vertical, and percent imbalances at all ROIs.	189
Table 4.12	GCP error for low tide data (2016).	190
Table 4.13	GCP error for low tide data (2017).	190
Table 4.14	Summary of horizontal and vertical accuracy for all epochs of UAV data collection.	191
Table 4.15	Vertical accuracy between UAV-DSM and GPS data.	192
Table 4.16	Vertical accuracy between the UAV-DEM (filtered DEM) and RTK-GPS data at ROI 6.	194
Table 4.17	Accuracy assessment of volumetric rates between the GCD method and erosion pin measurement during 2016-2017.	197
Table 4.18	Accuracy assessment of vertical change rates between the GCD method and erosion pin measurement during 2016-2017.	198

LIST OF FIGURES

FIGURE NO.	TITLE	PAGE
Figure 1.1	Mangrove forest distribution and extent in Peninsular Malaysia, Sabah, and Sarawak (Omar, Husin, and Parlan, 2020).	2
Figure 1.2	The threats to the mangrove ecosystem (IUHN, 2020).	6
Figure 1.3	The study area's location includes: (A) the location of Langkawi Island on a map of Peninsular Malaysia; and (B) the location of the Kilim River on a map of Langkawi Island.	16
Figure 1.4	General methodology of study.	18
Figure 2.1	A world map of the mangrove distribution zones and the number of mangrove species in each region (Deltares, 2014).	25
Figure 2.2	Riverine mangrove type (Hoff and Michel, 2014).	26
Figure 2.3	Fringe mangrove type (Hoff and Michel, 2014).	27
Figure 2.4	Basin mangrove type (Hoff and Michel, 2014).	28
Figure 2.5	The illustrations of the accretion and erosion processes and the related factors (McIvor et al., 2013).	29
Figure 2.6	The sight of the erosion process in a mangrove area within Kilim Karst Geoforest Park, Langkawi Island, Malaysia.	30
Figure 2.7	The Surface Elevation Table-Marker Horizon (SET-MH) apparatus during the process of measuring marsh (top right) and mangrove (bottom right) surface elevation (McIvor et al., 2013).	40
Figure 2.8	The interaction between mangrove surface elevation changes and sea level rise (McIvor et al., 2013).	44
Figure 2.9	UAV types (Chakrasthitha, 2015).	48
Figure 2.10	Observation of GPS positioning data (Blake, 2019).	53
Figure 2.11	UAV-RTK method for GPS positioning data observation (Blake, 2020).	54
Figure 2.12	UAV-PPK method for collecting GPS positioning data observation (Blake, 2020).	55

Figure 2.13	The basic workflow of SfM-MVS (Smith, Carrivick, and Quincey, 2016).	63
Figure 2.14	The example of DSM (GISGeography, 2022).	69
Figure 2.15	The DEM model of flat and mountainous surface of earth (GISGeography, 2022).	70
Figure 2.16	The DTM representation (GISGeography, 2022).	71
Figure 2.17	Different elevations are generated through multiple filtering algorithms in bare, shrub, and vegetation areas (Anders et al., 2019).	78
Figure 2.18	The concept of the SNERL filtering algorithm.	80
Figure 2.19	Schematic of the DoD concept underlying the GCD (ESSA, 2019).	82
Figure 2.20	Digital elevation models, precision maps, and LoD show the spatial distribution of the errors along the flume. Changes with a magnitude smaller than the LoD can be disregarded (Candido, 2019).	85
Figure 2.21	A workflow for producing a DEM of difference by applying probabilistic thresholding using a user-defined confidence interval (Williams et al., 2011).	87
Figure 2.22	An example of mapping spatial variability of DEM of Difference (DoD) uncertainty using multiple parameter combinations based on the three inputs (point density, slope, and GPS quality) in a three-rule fuzzy inference system to produce a defuzzified prediction of elevation uncertainty (Williams et al. (2011).	88
Figure 2.23	The conceptual framework of UAV capability helps mangrove surface elevation change monitoring at canopy-covered riverbanks.	96
Figure 2.24	The nearest opening to the bare earth surface is in the dense mangrove forest in the study area; (a) line profile at the orthophoto+UAV-DSM overlap image; (b) the height profile based on the established line profile.	97
Figure 3.1	The general methodology of the study (red dash-line and green highlight: objective of the study).	108
Figure 3.2	(A) Location of the study area in Malaysia's Peninsular (shown by the small yellow square); (B) Location of the Kilim River as the major study area displayed in the orthophoto image captured by the UAV; (C) Location of the study area on the map of Langkawi Island, Kedah, Malaysia (shown by the small yellow square).	111

Figure 3.3	The DJI Phantom 4 advanced as the platform for collecting aerial photographs over the Kilim River.	113
Figure 3.4	The flight path for each UAV data acquisition is based on plotted mission planning via device-DJI Go connected at different tides and times of the year.	115
Figure 3.5	(A) GCP distribution in the study area; (B) GCP observation at Stn 6 using the Topcon GR5 receiver; and (C) GCP observation at Stn 8 using the Topcon GR5 receiver (Mohamad et al., 2019).	117
Figure 3.6	The distribution of RTK-GPS points along the Kilim River has been measured using Topcon GR-5. Fourteen RTK-GPS validation points were created at the highlighted area (opening hole) in the middle of the mangrove forest in ROI 6.	120
Figure 3.7	The distributions of erosion pins along the entire Kilim River (A, B, C, D, and E in the red highlighted points refer to the main validation area, which is expected to have significant elevation changes, especially erosion rates); (E and F in the green highlighted points represent the erosion pins in the controlled area, which are supposed to have insignificant erosion but higher accretion rates.	121
Figure 3.8	Various perspective views of erosion pins at the Kilim riverbank sites (redrawn from Myers, Rediske, and McNair, 2019).	122
Figure 3.9	The specific image processing workflow for UAV data uses the SfM-MVS method.	123
Figure 3.10	Non-vegetation filtering workflow using a VI-based filtering technique.	127
Figure 3.11	The normalised differential vegetation index (NDVI) is used to classify vegetation and non-vegetation. (A) RGB image-based UAV flying over the Kilim River; (B) NDVI converted from RGB to vegetation colour index; and (C) binary vegetation and non-vegetation colour using the ExG greenness approach.	128
Figure 3.12	Non-vegetation features are removed using ExG features and UAV-DSM data. (A) ExG-derived integer; (B) ExG polygons converted to shapefile types; (C) extracted vegetation features; and (D) vegetation features clipped with UAV-DSM data.	129
Figure 3.13	The specific vegetation filtering workflow uses the SNERL filtering algorithm.	130

Figure 3.14	The specific vegetation filtering workflow uses the SNERL filtering algorithm.	132
Figure 3.15	The specific vegetation filtering workflow uses the SNERL filtering algorithm.	133
Figure 3.16	Identify the highest cluster of height by creating a profile line across vegetation with a hole opening.	134
Figure 3.17	Identifying the medium cluster of height.	135
Figure 3.18	Identifying a low cluster of height.	135
Figure 3.19	The vertical elevation of UAV-DSM data after the filtering process using the SNERL algorithm; (a) patch profile line, which is similar to the line created in Figure 3.13; (b) the histogram of final UAV-DEM height after the filtering process.	136
Figure 3.20	GCD workflow for the filtered DEM at low tide in 2016 and 2017.	138
Figure 3.21	The flow of the method for generating DEM change detection using GCD stand-alone software.	139
Figure 4.1	A flowchart of stage one processing (based on the general methodology in Figure 3.1).	146
Figure 4.2	Point cloud and dense cloud output using the SfM-MVS method; (a) during low tide (year 2016); (b) during low tide (year 2017).	147
Figure 4.3	Orthophotos and UAV-DSM results from SfM-MVS processing using Agisoft Metashape v1.6.4 software; (a) during low tide (year 2016); (b) during low tide (year 2017).	148
Figure 4.4	Camera locations and image overlap for UAV data collection in 2016 and 2017 at low tide conditions.	149
Figure 4.5	The image residuals for the FC330 sensor attached to the UAV Phantom 4 advanced.	151
Figure 4.6	Flowchart of stage two processing (refer to general methodology in Figure 3.1).	152
Figure 4.7	The result of non-vegetation removal using the normalised differential vegetation index (NDVI); (a) ROI during low tide 2016; (b) ROI during low tide 2017.	154
Figure 4.8	The result of non-vegetation removal using the normalised differential vegetation index (NDVI); (a) ROI during low tide 2016; (b) ROI during low tide 2017.	158

Figure 4.9	Over a one-year period (2016–2017), a comparison of the UAV-DEM based on average elevation height distribution in histogram and elevation legend at ROI 1 was made. The rest of the ROI comparisons were placed in Appendix F and G.	159
Figure 4.10	Profile line comparison between the filtered DEM at low tide in 2016 and at low tide in 2017.	164
Figure 4.11	A flowchart of stage three processing (based on the general methodology in Figure 3.1).	164
Figure 4.12	The result of change detection at different ROIs at Kilim River using GCD software: (a) ROI 1; (b) ROI 2; (c) ROI 3; (d) ROI 4; (e) ROI 5; (f) ROI 6; (g) ROI 7; (h) ROI 8.	167
Figure 4.13	GCD analysis of ROI 1: (a) areal changes, (b) volumetric changes, and (c) vertical averages. The remaining results of the GCD analysis were placed in Appendix H.	168
Figure 4.14	Vertical accuracy assessment between UAV-DSM and static GPS.	193
Figure 4.15	Flowchart of vegetation filtering assessment between UAV filtered DEM and RTK GPS (based on general methodology in Figure 3.1).	194
Figure 4.16	The correlation coefficient of the relationship between UAV-DSM and static GPS data.	195
Figure 4.17	Vertical accuracy assessment between the filtered DEM and static GPS.	196
Figure 4.18	A flowchart of stage three processing (based on the general methodology in Figure 3.1).	199

LIST OF ABBREVIATIONS

2D	-	Two Dimensional
3D	-	Three Dimensional
AEB	-	Auto Exposure Bracketing
ALSM	-	Airborne Laser Scanner Method
ANN	-	Approximate Nearest Neighbour
APV	-	Automatically Piloted Vehicle
ASIFT	-	Affine Scale Invariant Feature Transform
ATIN	-	Adaptive Triangulated Irregular Network
AUC	-	Area of Curve
BRIEF	-	Binary Robust Independent Elementary Features
CANUPO	-	CAractérisation de NUages de POints
CE	-	Conformité Européenne
CMOS	-	Complementary Metal Oxide Semiconductor
CMVS	-	Clustering Views for Multi-view Stereo
CNN	-	Convolutional Neural Networks
CPU	-	Central Processing Unit
CSF	-	Cloth Simulation Filtering
DEM	-	Digital Surface Model
DJI	-	Da-Jiang Innovations
DoD	-	DEM of Difference
DSM	-	Digital Surface Model
DSMM	-	Department of Surveying and Mapping Malaysia
DTM	-	Digital Terrain Model
EDM	-	Electronic Distance Measurement
EPSG	-	European Petroleum Survey Group
ETEW	-	Elevation Threshold with Expand Window
EVI	-	Enhanced Vegetation Index
ExG	-	Excessive Greenness
ExG-VI	-	Excessive Greenness Vegetation Index
EXIF	-	Exchangeable Image File

FAO	-	Food and Agriculture Organization
FCC	-	Federal Communication Commission
FDPM	-	Forestry Department of Peninsular Malaysia
FIS	-	Fuzzy Inferencing System
GCD	-	Geomorphological Change Detection
GCP	-	Ground Control Point
GDM	-	Geocentric Datum of Malaysia
GNSS	-	Global Navigation Satellite System
GPS	-	Global Positioning System
GPU	-	Graphics Processing Unit
HAT	-	Highest Astronomical Tide
HDR	-	High Dynamic Ranges
ICAO	-	International Civil Aviation Organization
IPM	-	Improved Progressive Morphological
ISL	-	Iterative Surface Lowering
ISL-VI	-	Iterative Surface Lowering – Vegetation Index
IUCN	-	International Union for Conservation Nature
KKGP	-	Kilim Karst Geoforest Park
LADA	-	Langkawi Development Authority
<i>LDAHash</i>	-	Linear Discriminant Analysis with Smaller Descriptors
LiDAR	-	Light Detection and Ranging
MCC	-	Multiscale Curvature Classification
MCO	-	Movement Control Order
ME	-	Mean Error
MLS	-	Maximum Local Slope
MinLoD	-	Minimum Level of Detection
MSL	-	Mean Sea Level
MVS	-	Multiview Stereo
MyGeoid	-	Malaysian Geoid Model
NAHRIM	-	National Water Research Institute of Malaysia
NDVI	-	Normalized Difference Vegetation Index
NFA	-	National Forestry Act
NFP	-	National Forestry Policy

NIR	-	Near-Infrared
NGM	-	National Geographic Magazine
PM	-	Progressive Morphological
PMF	-	Progressive Morphological Filter
PMVS	-	Patch-based Multi View Stereo
PPK	-	Post Processing Kinematic
PRF	-	Permanent Reserved Forests
PS	-	Agisoft Photoscan
RAM	-	Random Access Memory
RANSAC	-	Random Sample Consensus
RMSE	-	Root Mean Square Error
RMS	-	Root Mean Square
ROA	-	Remotely Operated Aircraft
ROC	-	Region of Curve
ROI	-	Region of Interest
RPA	-	Remotely Piloted Aircraft
RPAS	-	Remotely Piloted Aircraft System
RPAV	-	Remotely Piloted Aerial Vehicle
RPV	-	Remotely Piloted Vehicle
RSET- MH	-	Rod Surface Elevation Table-Marker Horizon
RSO	-	Rectified Skewed Orthomorphic
RTK	-	Real Time Kinematic
SD	-	Standard Deviation
SDE	-	Standard Deviation Error
SegTF	-	Segment-based Terrain Filtering
SET	-	Surface Elevation Table
SET-MH	-	Surface Elevation Table-Marker Horizon
SfM	-	Structure From Motion
SfM-MVS	-	Structure from Motion-Multiview Stereo
SIFT	-	Scale Invariant Feature Transform
SLR	-	Sea Level Rise
SLR	-	Single-lens Reflex

SMRF	-	Simple Morphological Filter
SNERL	-	Surface estimation from Nearest Elevation and Repetitive Lowering
SURF	-	Speeded Up Robust Features
TERRA	-	Terrain Extraction from Elevation Raster through Repetitive Anisotropic
TIN	-	Triangulated Irregular Network
TLS	-	Terrestrial Laser Scanner
UAS	-	Unmanned Aerial System
UAV	-	Unmanned Aerial Vehicle
UAV- DSM	-	Unmanned Aerial Vehicle – Digital Surface Model
UMA	-	Unmanned Aircraft
UNEP	-	United Nation Environment Programme
UNESCO	-	United Nations Educational, Scientific and Cultural
UVS	-	Unmanned Vehicle Systems
VDVI	-	Visible-band Difference Vegetation Index
VI	-	Vegetation Indices
VVI	-	Visible Vegetation Index
VTOL	-	Vertical Take-off Landing
WWF	-	World Wildlife Fund

LIST OF SYMBOLS

$\mathcal{E}r$	-	Rate of Erosion
σ	-	Standard Deviation Error
τ_e	-	The Effective Hydraulic Stress
τ_c	-	The Critical Stress
σ_Z	-	Vertical Standard Deviation
δZ	-	DEM uncertainty
η	-	Physical Properties of the Studied Surface
δ_E	-	DEM Change in Elevation
δz	-	Vertical Error Component
DEM_1	-	Previous/Past DEM
DEM_2	-	Newest//Current DEM
E_{GPS}	-	Y coordinate of GCP observed by GPS
E_M	-	Y coordinate on orthophoto
E_{rate}	-	Volumetric Rate of Erosion
g	-	Negative Residual
h	-	Ellipsoidal Height
H	-	Orthometric Height
$H_{a,b}$	-	Weight Value
H_i	-	Vegetation Height
H_1	-	Standard Deviation Error For Current DEM
H_2	-	Standard Deviation Error For Current DEM
H_{DSM}	-	UAV-DSM Measured Coordinate
H_{GPS}	-	GPS Observed Coordinate
H_i	-	Vegetation Height
K	-	Kappa Coefficient
kd	-	Erodibility or Detachment Coefficient
$K_{i,j}(\lambda, \eta)$	-	The Chosen Kernel Averaging Function
M	-	Mean
$ME_{N,E,H}$	-	Mean Error For Northing (N), Easting (E) and Orthometric height (H)

N	-	Geoid Height
N_{GPS}	-	X coordinate of GCP observed by GPS
N_M	-	X coordinate on orthophoto
n	-	Number of GCP
P_i	-	Weight of residual
$RMSE_E$	-	RMSE of Easting
$RMSE_N$	-	RMSE of Northing
$RMSE_Z$	-	RMSE of Elevation
S	-	Signal
SD	-	Standard Deviation Error
$SD_{N,E,H}$	-	Standard Deviation Error of GCPs For Northing (N), Easting (E) and Orthometric Height (H)
t	-	Critical t value
U_{crit}	-	Critical Threshold Error
VGC	-	Variability Due to Geomorphological Change
VE	-	Variability Caused by Error
V_{rate}	-	Vertical Average Changes

LIST OF APPENDICES

APPENDIX	TITLE	PAGE
Appendix A	GPS Observation - December 2016	253
Appendix B	GPS Observation - December 2017	269
Appendix C	Processing Parameters of UAV Data Collection based on the SfM-MVS Method using Agisoft Metashape v1.6.4	273
Appendix D	SNERL Filtering Procedure	277
Appendix E	SNERL Code	279
Appendix F	Comparison Between Unfiltered and Filtered UAV-DEM (2016)	281
Appendix G	Comparison Between Unfiltered and Filtered UAV-DEM (2017)	289
Appendix H	Geomorphological Change Detection (GCD) Results for the Remaining ROIs	297

CHAPTER 1

INTRODUCTION

1.1 Background of Study

Mangrove forests serve as one of the most productive and biologically diverse ecosystems on the planet. Mangrove forests are found along sheltered coasts where they grow abundantly in saline soil and brackish water, subject to periodic fresh-and-salt-water inundation. Mangrove trees have unique characteristics such as rigid root systems, striking bark and leaf structures, and other adaptations that allow them to survive in harsh conditions in their habitat (WWF, 2020). The habitat is soft, silty, and shallow, coupled with the endless ebb and flow of water, providing very little support for most mangrove plants, which have aerial or prop roots (known as pneumatophores, or respiratory roots) and buttressed trunks. It is critical to human well-being because it provides basic necessities such as food, shelter, and employment. Mangroves reduce the loss of property and the vulnerability of local communities.

Mangrove forests play a dynamic role in maintaining the sustainability of the environment, biodiversity, and environmental values. Mangrove forests protect coastlines against erosive wave action and strong coastal winds, and they serve as natural barriers against tsunamis and torrential storms. Furthermore, the mangrove forest acts as a climate regulator, absorbing up to four times more carbon dioxide than upland terrestrial forest areas (Donato et al., 2011). Mangrove trees protect coastal areas from storm surges and tsunamis by lowering the magnitude of the big waves by half or three-quarters (Onrizal et al., 2017). In a prior study in Vietnam (Bao, 2011), the lowering of the wave was found to increase with the height of the water. Another study discovered that mangrove forests have the ability to generate "living seawalls," which are more cost-effective in terms of coast protection than concrete seawalls and other man-made structures (Ca and Xuyen, 2008). Mangrove trees can adapt to sea

level dwellings and interact effectively with tidal fluctuations when it comes to sea level increase.

In the year 2017, Malaysia had a total of 629,038 hectares (ha) of mangrove forest, with Sabah comprising 60%, while the remaining 22% and 18% were spotted in Sarawak and Peninsular Malaysia (Figure 1.1). The total mangrove area for Sabah is 378,195 ha, while for Sarawak and Peninsular Malaysia, it is 139,890 ha and 110,953 ha. Mangroves in Peninsular Malaysia have been found on the sheltered west coast that borders the Straits of Malacca in the states of Kedah, Perak, Selangor, Melaka and Johor. Meanwhile, in Sabah, mangroves are mostly in Pedalaman, Pantai Barat, Kudat, Sandakan, and Tawau. In Sarawak, the mangroves are mostly populated in Kuching, Samarahan, Sri Aman, Sarikei, Sibuan, and Limbang. The largest mangrove forest occurs in Perak, which covers about 38% of the total mangrove area found in Peninsular Malaysia, followed by Johor, Selangor, Pahang, Kedah, Terengganu, Negeri Sembilan, Pulau Pinang, Melaka, Kelantan, and Perlis. The distribution of mangroves that occur along Peninsular Malaysia, Sabah, and Sarawak's coastlines is depicted in Figure 1.1.

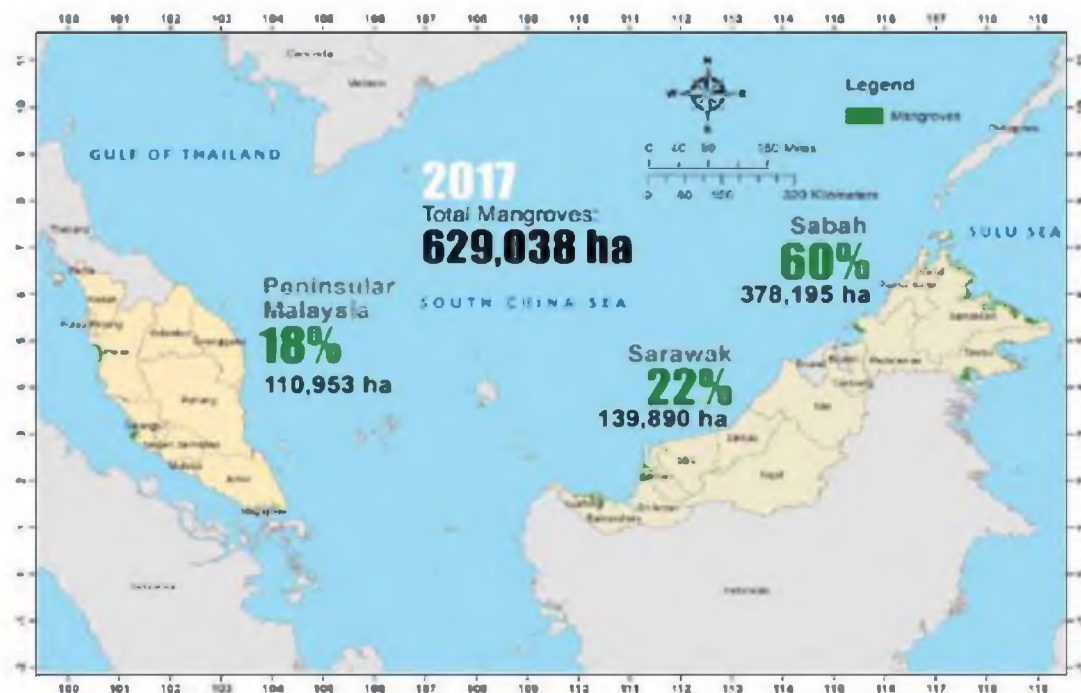


Figure 1.1 Mangrove forest distribution and extent in Peninsular Malaysia, Sabah, and Sarawak (Omar, Husin, and Parlan, 2020).

Between 1990 and 2020, the global area of mangroves shrank by 1.04 million ha (Table 1.1). Over the last three decades, the rate of loss has decreased by more than half, from 46,700 ha per year in 1990–2000 to 36,300 ha per year in 2000–2010 and 21,200 ha per year in the most recent decade. In Africa, the average annual rate of loss decreased from 6610 hectares in 1990–2000 to 2330 hectares in 2010–2020. Oceania has seen a decrease in the rate of loss, from 29,600 ha per year in the 1990s to 5,900 ha per year in the last decade. There was an increase in mangroves in South America in 2010–2020 at an average annual rate of 14,800 ha, reversing the declining trend in 1990–2000, when the region lost mangroves at a rate of 10200 ha per year. Mangrove areas increased at a rate of 10,500 ha per year on average in North and Central America from 2010 to 2020 (with only a minor change between 1990 and 2010). The increase in the region from 2010 to 2020 was largely due to Cuba, which gained 12,000 ha per year throughout that time. This increase, like in Guyana, is attributable to improved data collection and restoration programmes and does not reflect genuine changes in mangrove acreage. The average yearly rate of mangrove loss in Asia increased dramatically from 1,030 ha in 1990–2000 to 38,200 ha in 2010–2020. Indonesia, which recorded an average yearly loss of 6,800 ha from 1990 to 2000 and 21,100 ha in the most recent decade, was primarily responsible for the increased rate of loss.

In Malaysia, the area of mangroves decreased from 65,0311 ha in the year 1990 to 642,063 ha in the year 2000 (Table 1.2). Meanwhile, in the year 2020, the number keeps shrinking from 642,063 in the year 2000 to 629,038 ha. The changing pattern of mangrove extent seems consistent from 1990 to 2000 and 2000 to 2020 (Omar et al., 2020). Between 1990 and 2000, the mangroves lost 8,248 ha, while the next 20 years showed another loss of mangroves at 13,025 ha. In Peninsular Malaysia, the mangrove pattern is changing from 116,746 ha in 1990 to 114,353 ha in 2000, while in 2020, the number will keep shrinking to 110,953 ha. For Sabah, the number also keeps shrinking, from 385,630 ha in 1990 to 382,448 ha in 2020, while in 2020, the mangrove area will change to 378,195 ha. In Sarawak, the mangroves changed from 147,936 ha to 145,263 ha, and in 2020, the mangrove area will be 139,890 ha. The number of mangrove losses is frightening, and the likelihood of the number remaining lower in the future is higher if the authorities ignore the mitigation plan.

Table 1.1 Trends in the area of mangroves by region, 1990–2020 (retabulated from FAO, 2020).

Region / Sub-region	Area of mangroves ('000 ha)			
	Year			
	1990	2000	2010	2020
Total Africa	3398	3332	3264	3240
(East Asia)	24	22	25	32
(South and Southeast Asia)	6117	6108	5713	5330
(Western and Central Asia)	190	190	190	184
Total Asia	6331	6320	5928	5545
Total Europe	0	0	0	0
(Caribbean)	787	789	774	891
(Central America)	492	482	483	466
(North America)	1152	1167	1190	1195
Total North and Central America	2431	2439	2447	2552
Total Oceania	1447	1150	1314	1255
Total South America	2152	2050	1976	2124
World	15759	15292	14928	14717

Table 1.2 The extent of mangroves in Malaysia (retabulated from Omar et al., 2020).

Region	Mangroves 1990 (ha)	Mangroves 2000 (ha)	Mangroves 2020 (ha)
Peninsular Malaysia	116,746	114,353	110,953
Sabah	385,630	382,448	378,195
Sarawak	147,936	145,263	139,890
Total	650,311	642,063	629,038

Mangrove degradation is related to natural and anthropological factors (Jusoff, 2013; Abd. Shukor, 2004). The natural factors comprised soil erodibility, riverbank slope, the velocity of water flow, water runoff, rainfall intensity, and harsh climate conditions. In another way, anthropological factors affect the mangrove through coastal development, aquaculture, agriculture, pollution, boat wake effects, sea level rise (SLR), and logging activities, as shown in Figure 1.2. Mangrove degradation is a complex issue because some researchers discovered that it is an apparent human-made factor that affects the mangrove ecosystem instantly, much like coastal development that instantly wipes out the mangrove population. Other factors, such as boat wake and SLR, are less well known as man-made factors that gradually impact the mangrove population. Boat wake and SLR factors might look less harmful, but they are far more dangerous because the effect is not instantaneous, and it causes mangrove degradation in a long-term way.

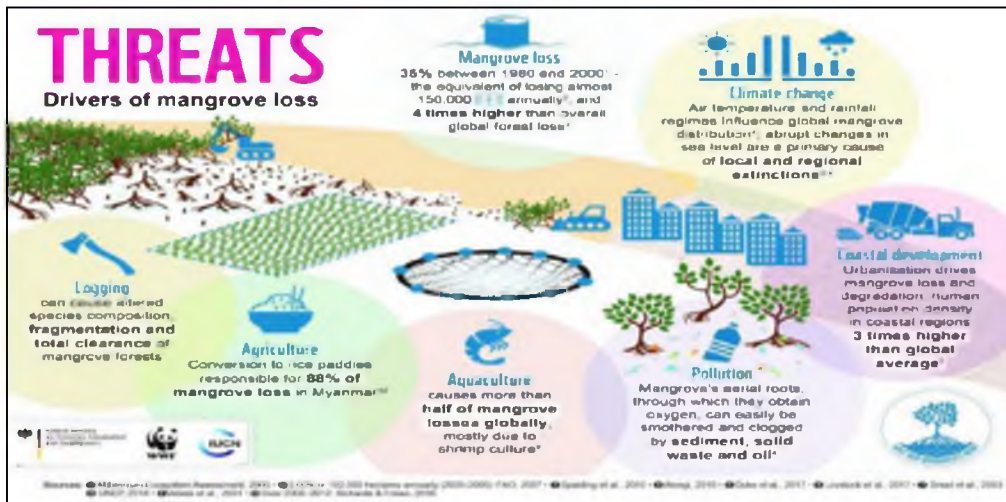


Figure 1.2 The threats to the mangrove ecosystem (IUHN, 2020).

Long-term mangrove degradation affects the mangrove population by changing the surface elevation, especially at the riverbank, through surface processes that comprise erosion, accretion, and sedimentation (McIvor et al., 2013). Erosion is the loss of surface material caused by water flows shearing off the top layer of the sediment surface, resulting in a loss of height. When the deposited material becomes cemented in place, it is called an accretion (the tides or waves can no longer wash it away). The deposition of inorganic sediments and organic debris on the surface is referred to as sedimentation. The deposited material can be allochthonous (i.e., from outside the mangrove area) or autochthonous (i.e., from within the mangrove area) (i.e., created within the mangrove area). These surface processes usually take time to change the mangrove surface elevation, and the effect is not as apparent as other mangrove threats, such as coastal development and logging. Still, it could cause mangrove degradation, and if neglected, more hectares of the mangrove population will disappear in the next decades.

This study uses vegetation filtering and geomorphological change detection (GCD) analysis from unmanned aerial vehicle (UAV) data to estimate surface elevation changes underneath the mangrove canopy. A novel method named "Surface estimation from Nearest Elevation and Repetitive Lowering (SNERL) filtering" has been developed to remove the mangrove canopy that covers the riverbank surfaces. The filtering method used the identified nearest surface level based on visible vegetation index (VVI) classification and repetitive lowering filtering to estimate the

elevation underneath the mangrove canopy. The filtered features would be a bare surface on which the elevation is referred to as the nearest identified elevation. Integrating UAV photogrammetry data, a novel SNERL algorithm and volumetric analysis from geomorphological change detection (GCD) could evaluate surface elevation changes underneath the mangrove canopy in intensive ways. This study contributes to new knowledge and enables the beneficiary to understand this issue profoundly and might assist in any mitigation plan in the future.

1.2 Problem Statement

Most previous surface extraction research has focused on surface elevation and surface change monitoring of the bare earth topography. The studies by Maktav, Erbek, and Kabdasli (2002); Sesli et al., (2009); Jayson-Quashigah, Addo, and Kodzo, (2013); Tamassoki, Amiri, and Soleymani, (2014); Aryastana, Ardantha, and Candrayana, (2018); Ragia and Krassakis (2019) and Ragia and Krassakis (2019) use satellite imagery to monitor erosion in the coastal region. Meanwhile, Casado et al., (2015); Neugirg et al., (2016); Wang et al., (2016); Hamshaw et al., (2017); Duro et al., (2018); Hemmelder et al., (2018); and Hamshaw et al., (2019) used UAV imagery to assess erosion in bare earth areas. The previous scholar monitors the erosion based on the visible changes in topography based on the bare Earth's spatial and temporal analysis. Previous researchers had made fewer attempts to evaluate the surface elevation changes caused by erosion, accretion (deposition), and sedimentation rates at riverbank areas covered by canopies or trees. At the canopy-covered riverbank area, the canopy has obstructed the surface, especially from an aerial view. The mangrove canopy covering the riverbank should be removed using the vegetation filtering method to monitor erosion in the canopy-covered area.

For a bare earth area like a coastal or open riverbank, any geomorphological changes are easily detected using several image analyses, such as change detection, image classification, thresholding and other remote-sensing related methods (Jayappa, Mitra and Mishra, 2006; Ghanavati et al., 2008; Kuleli et al., 2011; Anders, Seijmonsbergen and Bouten, 2013; Guimarães et al., 2014; Ramirez-Cuesta et al.,

2016; Kaliraj, Chandrasekar and Ramachandran, 2017; Cook, 2017; Le Mauff et al., 2018). Both satellite imageries provided high resolution elevation data at the global scale and were used by previous researchers to evaluate changes on the Earth's surface over time (Nikolakopoulos, Kamaratakis, and Chrysoulakis, 2006; Siart, Bubenzer, and Eitel, 2009; Hirt, Filmer, and Fetherstone, 2010; Forkuor and Maathuis, 2012; Gesch, Oimoen, and Evans, 2014; Jing et al., 2014; Yue et al., 2017 and Elkhachy, 2018). Most of them used the DEM uncertainty process based on the Monte Carlo approach (James, Robson, and Smith, 2017) with post-processing tools in SFM-georeferencing software (James and Robson, 2012). Precision maps were created by interpolating the vertical standard deviation (H) determined from the precision estimate (1-mm grid size) (Taylor, 1997; Brasington, Langham and Rumsby, 2003; Lane, Westaway and Murray Hicks, 2003; and Wheaton et al., 2010).

Mangrove canopy covering is the main issue in this study, since it conceals the riverbank topography structures underneath. Physical erosion monitoring in the canopy-covered area is challenging to detect because of harsh mangrove environments and ecosystems such as route accessibility, tidal influence, and difficulty setting up surveying instruments in muddy and root-complex conditions (Kuenzer et al., 2011; Azian and Mubarak, 2012). Total stations, terrestrial laser scanners (TLS), electronic distance measurement (EDM), and other surveying equipment that needs a tripod are hardly set up in this terrain. The alternative way to monitor erosion in the mangrove environment is to use mangrove boundary/vegetation line shifting, such as that discovered by Mohamad et al. (2017); (2018); and (2019). The study, however, only examines the surface of the mangrove canopy and ignores the hidden features beneath it. Any physical changes on the ground are hidden by mangrove vegetation, especially from an aerial view, and these obstacles have inspired this study. A few terrestrial measurements, including physical surveys, erosion pins, and the SET-MH method, commonly quantify surface elevation changes. However, aerial monitoring is still convenient compared to terrestrial monitoring in terms of mobility, time-consuming, data abundance, and the ability to cover a large area in a short time. Besides, tidal inundation in mangrove areas that often becomes a problem for researchers (if using a physical survey method) could be avoided using the aerial monitoring method (Kanniah et al., 2015; Wang et al., 2019).

Researchers have developed many filtering methods to remove above-ground objects such as vegetation, buildings, and other human-made structures for decades. Filtering approaches such as LAStools triangulated irregular networks (TIN) densification, the typical method in Agisoft Photoscan (PS), and others have been used to filter point clouds by utilising light detection and ranging (LiDAR) (Yilmaz and Gungor, 2018; Anders et al., 2019; Zeybek and Şanlıoğlu, 2019). Similar to UAV imagery data, it uses several algorithms, for instance, a progressive morphological filter (PMF), a simple morphological filter (SMRF), or a cloth simulation filter (CSF), and a structural filter, CANUPO (CAracterisation de NUages de POints) for vegetation filtering purposes (Stroner et al., 2021). Unlike LiDAR, a UAV photogrammetric survey could not penetrate partly through the vegetation layer and, therefore, might have failed to generate actual ground points underneath a vegetated surface. The aerial photograph could not capture the information underneath dense vegetation using a typical sensor (e.g., RGB sensor) unless the captured RGB images are analysed using a specific method, like an excessive greenness vegetation index (ExG-VI), for surface extraction in dense forest areas (Anders et al., 2019). Even though sensor technologies rapidly grow every day, getting the surface information underneath the tree is still challenging if the filtering technique is unsuitable for the environment. Anders et al. (2019) also evaluated the comparison of DEM accuracy using common filtering algorithms such as the standard method in Agisoft Photoscan (PS), colour-based filtering using an excessive greenness vegetation index (VI), iterative surface lowering (ISL), triangulated irregular network densification from LAStools (TIN), and a combination of iterative surface lowering and the VI method (ISL+VI).

Hence, this study focuses on improving the vegetation filtering algorithm for extracting the surface elevation underneath the mangrove canopy to form a novel algorithm called Surface estimation from Nearest Elevation and Repetitive Lowering (SNERL). This algorithm was chosen due to its capability to reduce mangrove canopy height to terrain level and then generate an unmanned aerial vehicle-digital elevation model (UAV-DEM) with an accuracy comparable to physical measurements, such as total station, leveling, or the Global Positioning System (GPS). The vertical datum underneath the mangrove canopy is based on the nearest identified surface level, such as a riverbank or opening surface in the middle of a dense vegetation area. The unmanned aerial vehicle-digital surface model (UAV-DSM), which represents

elevation at mangrove canopy height, has been collected from UAV data that comprises two different flying durations, during low and high tide. UAV raw data (in the form of raw aerial images) is processed based on the structure from motion (SfM-MVS) method using commercial software such as Agisoft Metashape. Although it can generate orthophoto, contours, and three-dimensional (3D) models, the UAV-DSM is the most crucial output in this study, with the other outputs, such as orthophoto, serving as supporting data. Since the UAV-DSM only captures the top of topographic features such as vegetation and buildings, it needs a filtering method to filter and reduce it until it reaches terrain level (ground surface). This study requires additional data, such as physical topographic data from RTK-GPS observations, to validate the accuracy of the filtered UAV-DEM.

1.3 Research Question

The first objective is to discover the vegetation filtering algorithm for estimating the surface elevation underneath the mangrove canopy. The first objectives have been supported by:

- i. Why is this filtering algorithm considered a novel approach? How is it different compared with the other approaches?
- ii. How does the SNERL algorithm reduce vegetation surface height until it achieves the surface elevation level?

The second objective is to generate a digital elevation model (DEM) underneath the mangrove canopy with vertical accuracy comparable to physical topography measurement. The following research question supports the implementation of the second objective:

- i. Why is the SNERL algorithm capable of generating such high accuracy in the filtered output?
- ii. How is vertical accuracy assessment made on the filtered DEM?

The third objective is to evaluate the rates of surface elevation changes using a geomorphological change detection method. The research questions supporting this objective are:

- i. What is the method for quantifying the rate of surface elevation change in the study area?
- ii. How does GCD analysis determine the region that experienced a severe surface elevation change?

The fourth objective is to correlate the interactions between mangrove surface elevation changes and sea level rise. The research questions supporting this objective are:

- i. What is the impact of geomorphological changes on mangrove geomorphology and the interactions with sea level changes?

1.4 Aim and Objectives of Study

The aim of the study is to estimate surface elevation changes underneath the mangrove canopy using vegetation filtering and the geomorphological change detection (GCD) method on unmanned aerial vehicle (UAV) data. This study is supported by four objectives:

- i. To discover vegetation filtering algorithms for estimating surface elevation underneath the mangrove canopy;
- ii. To generate a digital elevation model (DEM) underneath the mangrove canopy with vertical accuracy comparable to physical topography measurement;

- iii. To evaluate the rates of surface elevation changes using geomorphological change detection method;
- iv. To correlate the interactions between mangrove surface elevation changes and sea level rise.

1.5 Significance of Study

The significance of the study is as below:

- Improving the existing filtering algorithm.
- Vertical datum identification underneath mangrove canopy.
- Highlighting the importance and the contribution of mangrove forest.

1.5.1 Improving the Existing Filtering Algorithm

This study presents new knowledge by improving the existing filtering algorithm from UAV aerial photogrammetry products to monitor the surface elevation changes underneath the mangrove canopy. The major challenge in this study is the part of filtering mangrove-covered riverbanks to generate actual surface elevation. Several algorithms in the past, like morphological filtering, multi-scale curvature classification (MCC), surface-based filtering, LasTool-LasGround module, progressive TIN Algorithm, and cloth simulation filtering (CSF), are effective in filtering unwanted features on the ground and have been well-proven in certain study areas. However, some algorithms are not suitable for the mangrove ecosystem environment, which is dense at the canopy and has a complex understory element. Hence, this study attempts to develop a novel algorithm to filter and extract surface from the mangrove canopy based on the nearest identified surface level as the referenced vertical datum. This algorithm improves the filtering process for extracting the surface elevation underneath the mangrove canopy to form a novel algorithm called Surface Estimation from Nearest Elevation and Repetitive Lowering (SNERL). This filtering algorithm

removes the mangrove canopy from the terrain level. It then generates a DEM whose accuracy is almost comparable to the physical measurement, using total station, levelling, or the Global Positioning System (GPS).

1.5.2 Vertical Datum Identification Underneath Mangrove Canopy

The major issue in this study is the position of the vertical datum at surface level, which is located underneath the canopy. In mangrove terrain, which is full of roots, mangrove seedlings, muddy soil, and other understory features, it is hard to identify the vertical datum of surface elevation except by using physical measurements like surface elevation table-marker horizon (SET-MH) and topographic surveys using total station or electronic distance measurement (EDM). Recently, the advancement of technology such as UAVs has revolutionised the way of mapping the earth's topography. The lower cost of purchasing, maintaining, and upgrading a UAV sensor compared to an airborne sensor is why this technology is gaining traction, particularly in mapping and geospatial applications. In this study, an actual terrain surface underneath the mangrove canopy will be displayed in the DEM model. To generate an actual elevation on the ground, the DEM model would be filtered using a filtering algorithm that has been developed to remove the mangrove canopy and the complex structure underneath, such as roots, mangrove seedlings, and muddy soil. The vertical datum underneath the mangrove canopy is based on the nearest identified surface level, such as a riverbank or opening surface in the middle of a dense vegetation area. The vertical datum is based on the nearest open surface in a dense mangrove forest, such as the bare riverbank or a falling tree that reveals the surface elevation. This opening surface will be the key element in the proposed filtering algorithm for interpolating the entire elevation area.

1.5.3 Highlighting the Importance and the Contribution of Mangrove

The last significance of the study is to highlight the importance and the contribution of mangrove forests, especially to humans. Mangroves play a dynamic

role in maintaining the sustainability of the environment, biodiversity, and economic values. In terms of environmental sustainability, mangroves protect the coast by lowering wave height by up to 66%, reducing erosion and flood risk in the coastal region. Mangroves are also carbon sinks, storing three to five times more carbon per hectare than tropical rainforests. Mangroves are considered a wildlife habitat for various species of animals, whether on land or in the water, and thus contribute to biodiversity conservation. It is also important as they provide a natural habitat for numerous species of fish, prawn, crab and other species that are dominant in muddy estuary areas. Mangroves are considered fish factories for the 210 million people who live and depend on them for food. Regarding economic value, mangroves contribute by providing eco-tourism activities that generate income for the locality, government agency, and whole country. In this study area, eco-tourism is the major contribution to the local economy as it helps create jobs, boosts the existing eco-tourism-based economy, and attracts domestic and international tourists to Langkawi Island. Mangrove forests are also valuable for charcoal and timber industries as they provide a source for manufacturing. Due to their endurance, tenacity, and hardness to water, mangrove trees receive high demand for their charcoal and timber sectors, which could therefore bring economic value for the country. Hence, this study will explore the relationship between human need, mangrove contribution and its correlation impact for short and long-term periods.

1.6 Scope of Study

The scope of study answers a few questions, including "what," "where," "when," and "how" the research was undertaken. "What" refers to the data that was utilised as the study's input. "Where" refers to the location of the case study area, which was chosen based on a number of factors. "When" refers to the start and completion of the study period as well as the time when data is collected. The term "how" refers to the process and method used to generate output and determine whether or not the objectives are attainable.

1.6.1 ‘What’ – Data and Equipment

This study focuses on UAV data as the primary data and GPS vertical data as the secondary data. The Phantom 4 Advanced model from Da-Jiang Innovations (DJI) was employed in this study. It has been chosen for this study due to its low cost of purchase and maintenance, its built-in RGB sensor, and its photogrammetry-friendly capabilities. A previous researcher conducted less research on the filtering process of mangrove vegetation using red, blue, and green (RGB) sensors and photogrammetry-based surveying. The UAV photogrammetry data includes orthophoto, point cloud data, 3D models, DSMs, and DEMs. UAV data is chosen instead of satellite images because low altitude data capture requirements range between 100 and 300 m for low altitude. The lower the flying altitude, the better the output data captured by the UAV with higher resolution. In addition, fewer fatalities occur if a crash happens at a low altitude. The UAV is also chosen as a data source because the pilot can fly the UAV while selecting the appropriate weather conditions to avoid any worsening incidents. Previous researchers chose small-scale photogrammetric mapping related to the surface elevation of a river or coastal area due to DTM accuracy of less than 10 cm (Flener et al., 2015). For UAV-DSM in small scale areas, the study by Uysal, Toprak, and Polat (2015) discovered its vertical accuracy at 6.62 cm. The UAV-DSM products serve as an altimeter for determining sea level changes throughout various tidal phases, with vertical precision of ± 0.50 m (50 cm) (Mohamad et al., 2019).

1.6.2 ‘Where’ – Location of Study Area

The study area was chosen to be a specific section of the Kilim River in the north-eastern part of Langkawi Island, Kedah, Malaysia, in order to adapt the UAV capability to capture data on a small scale (Figure 1.3). The study area is within the Kilim Karst Geoforest Park (KKGP). This geoforest park is being granted by the United Nations Educational, Scientific, and Cultural Organization (UNESCO) because of its fascinating rock formations (limestone or karst) and its unique geological significance. This area was chosen because of the richness of the mangrove forest that hides the terrain underneath. The mangrove tree, which is dense and complicated,

especially the understory features of mangrove morphology (i.e., roots, bark, and soil formation), has inspired the objective of this study. However, because of the limitation of UAV capabilities to cover all parts of KKG, only a small part of the Kilim River was chosen. The study area only covers 0.649 kilometres of KKG and is located approximately 1.7 kilometres from the coast. The traffic conditions in this area are intense and busy because of the tourism factor, which strengthens this selection of study areas. The traffic factor also becomes a catalyst factor that changes the surface elevation at the riverbank, and the possibility of this study area showing a clear change trend is higher than the other parts of KKG. More discussion on the study area has been explained in Sub-section 3.3 in Chapter 3.

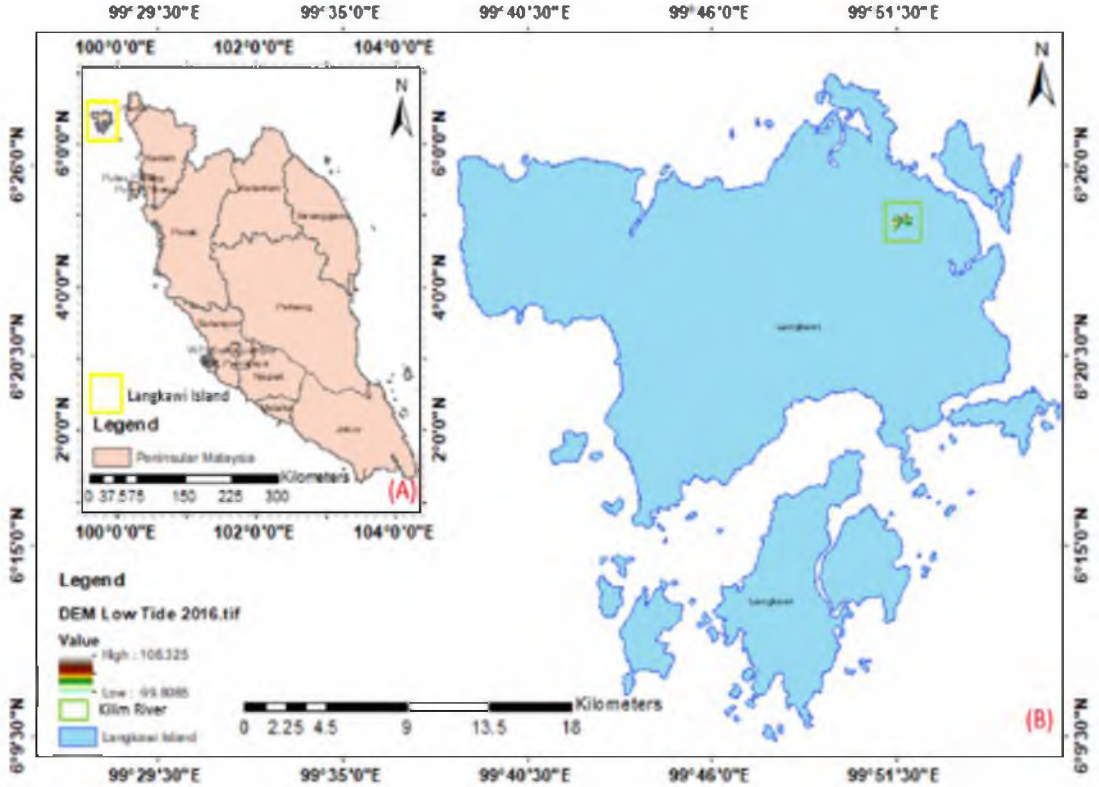


Figure 1.3 The study area's location includes: (A) the location of Langkawi Island on a map of Peninsular Malaysia; and (B) the location of the Kilim River on a map of Langkawi Island.

1.6.3 ‘When’ – Duration of Study and Date of Data Taken

The duration of the study is approximately one year, starting from the year 2016 until 2017. For the year 2016, the data collection comprised UAV data acquisition, which is carried out during low tide conditions. Then, a similar process was repeated in the year 2017. The reason for flying the UAV during low tide conditions is to avoid tidal influence, especially during high tide. Both flights captured data in the same study area, which is the Kilim River. The time interval between the first and second epochs of data acquisition in one year is to get the short-term impacts of surface elevation change components (erosion, accretion, and sedimentation) and the rate of changes within a one-year interval. Since many studies have been conducted based on the long-term impact of surface elevation changes (especially erosion and accretion), this study attempts to study the mangrove ecosystem based on its short-term impact.

1.6.4 ‘How’ – Methodology and Technique

The focus of this study comprises three stages. The first part is UAV image processing based on the structure of the motion-multiview stereo (SfM-MVS) algorithm using Agisoft Metashape software. The SFM-MVS workflow starts with image loading and alignment, followed by ground control point (GCP) data insert and camera and image optimisation. The last process of the SfM-MVS method is constructing the point cloud, building the mesh, and texturing the model. The output of this process comprises orthophoto, DSM, 3D model, tiled model, point cloud data, contours, and a quality report. In stage two, the filtering process is to extract surface elevation from the mangrove canopy. The filtering process used a novel algorithm developed based on filtering and extracting surface from mangrove canopy from the nearest identified surface level as the referenced vertical datum. The last stage is the evaluation of surface elevation changes, which includes erosion, accretion, and sedimentation, using the geomorphological change detection (GCD) method. The GCD method uses DEM of difference (DoD) and a few other analysis tools to evaluate and display models for each surface elevation change process.

1.7 General Methodology

The study is divided into six major sections: literature review, study area selection, data acquisition, data processing, data analysis, and study output (Figure 1.4). A literature review is a part of revising the past related studies and extracting the relevant information to search for the novel for this study. Then, the selection of the study area is a part of when the criteria of certain places are being evaluated to fulfil the requirements of this study, where the area has significant value in terms of geography, geology, demography, and geomorphology. The next part of the methodology is data acquisition, which is one of the crucial elements in this study. The chosen data should be capable of processing, analysing, and visualising the findings of the study. Data also needs to be measurable and achievable to avoid delays in further methods. The other part of the general methodology shows the data processing that is important to generate the result for further discussion and analysis. Data processing involves data manipulation using a specific method to produce a quality and accurate result. Furthermore, data analysis is required to analyse the results and discuss the findings. The analysis determines whether the result is accurate before reaching the last method, which is the visualisation of the output of the study. More information about the methodology of the study can be found in Chapter 3.

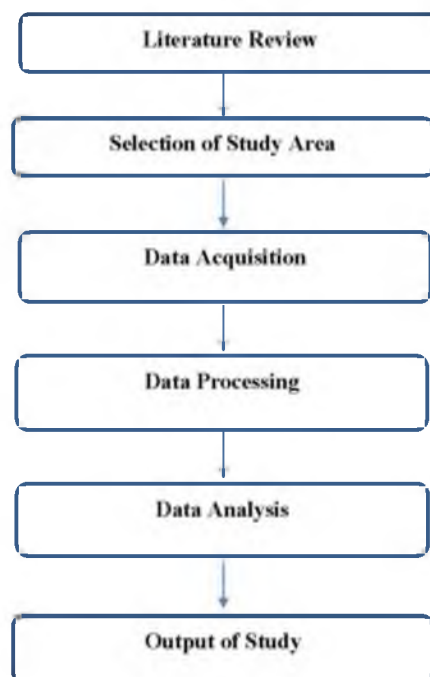


Figure 1.4 General methodology of study.

1.8 Thesis Outline

This research is divided into five chapters. This chapter provides an overview of the study, including its background, problem statement, aims and objectives, research question, significance, scope and limitations, and general methodology. For the scope of the study section, it comprises a few questions such as "what" to justify certain data and equipment, "where" to clarify why certain study areas were chosen, "when" to explain the duration of the study and period of data acquisition, and last, "how" to describe the method and technique that were used in this study.

Chapter 2 debriefs the literature review of this study, which comprises an introduction to the mangrove ecosystem, mangrove surface elevation changes and their factors, an overview of UAV, the elements of digital photogrammetry and the SfM-MVS concept, vegetation filtering from UAV-based photogrammetry data, quantification of surface elevation changes using geomorphological change detection (GCD) analysis, and a summary of the key literature review. In Section 2.2 (mangrove ecosystem), the explanation comprises an overview of the mangrove ecosystem and mangrove surface topographies and landform types. Then, in Section 2.3 (mangrove surface elevation changes and their factor), the topic contains the definition of mangrove surface elevation changes and their process, the factor of mangrove surface elevation changes, and previous studies related to the physical measurement of surface elevation changes. Meanwhile, in Section 2.4 (an overview of UAV), the sub-section discusses the introduction to UAV and its terminology, the history and development trend of UAV, the types of advantages and disadvantages of UAV, and the elements of the positioning system in UAV mapping. In Section 2.5 (the elements of digital photogrammetry and the SfM-MVS concept), the topics involve an overview of digital photogrammetry; an overview of SfM-MVS in digital photogrammetry; and principles of SfM-MVS. Following that, Section 2.6 (Vegetation filtering from UAV-based photogrammetry data) includes an overview of vegetation filtering from UAV-based photogrammetry, previous studies related to vegetation filtering technique, vegetation index (VI) for segregating vegetation and non-vegetation areas, and surface estimation from nearest elevation and repetitive lowering (SNERL) algorithm at mangrove vegetation area. Subsequently, for Section 2.7 (the quantification of surface elevation

changes using geomorphological change detection (GCD) analysis), the section comprises an overview of geomorphological change detection (GCD), DEM of difference (DoD), DEM error assessment, and previous studies related to the GCD quantification method. Section 2.8 (summary of key literature reviews) comprises a critical review of the previous study and the novelty and contribution of this study.

Chapter 3 describes the methodology of this study. The chapter started with the introduction, methodology, study area, data collection, data processing, data analysis, and the output of the study. In Section 3.4 (data collection), the section explained UAV and GPS data acquisition. Section 3.5 (data processing): the section discussed the SfM-MVS workflow, segregation of vegetation and non-vegetation areas using vegetation indices (VI), vegetation filtering using the SNERL algorithm, and quantification of surface elevation changes using the geomorphological change detection (GCD) method. Section 3.6 (data analysis) comprises accuracy assessment for GCPs, accuracy assessment of UAV-DSM (unfiltered DEM), and accuracy assessment of UAV-DEM (filtered DEM). Section 3.7 (output of the study) explains briefly the results that will be generated in the next chapter.

Chapter 4 emphasises the results and analysis in this study. The chapter outlines the introduction, results of SfM-MVS processing, results of vegetation filtering processing, results of geomorphological change detection (GCD) processing and analysis, and, lastly, discussions. For Section 4.2 (results of SfM-MVS processing), the section highlights UAV survey parameters, UAV survey results, and camera calibration results. Meanwhile, Section 4.3 (results of vegetation filtering processing) discusses non-vegetation removal results using vegetation index (VI) filtering and vegetation filtering results using the SNERL algorithm. Section 4.4 (the result of geomorphological change detection (GCD) processing) explains qualitative and quantitative analysis of GCD output for regions of interest (ROIs). In Section 4.5 (analysis), the section focuses on the accuracy assessment of GCPs, UAV-DSM (unfiltered DEM), UAV-DEM (filtered DEM), and GCD-erosion pin rates. Based on these findings, in Section 4.6 (discussion), the section emphasises geomorphological changes underneath the mangrove canopy at Kilim River. Section 4.6 also discussed

the short- and long-term impacts of geomorphological changes on the mangrove surface and their interaction with sea level rise.

Chapter 5 concluded the whole study based on the findings and analysis of this study. The chapter outlined the introduction, fulfilment of objective and research questions, recommendations for future study, and conclusion.

REFERENCES

- Abd Elbasit, M.A., Anyoji, H., Yasuda, H. and Yamamoto, S. (2009) 'Potential of low cost close-range photogrammetry system in soil microtopography quantification', *Hydrological Processes*, 23, 1408–1417. <https://doi.org/10.1002/hyp.7263>.
- Abd, Shukor. A.H. (2004). 'The use of mangrove in Malaysia, In: Promotion of mangrove-friendly shrimp aquaculture in Southeast Asia', Tigbauan, Iloilo, Philippines: Aquaculture Department, Southeast Asian Fisheries Development Center, 136-144.
- Adame, M.F., Neil, D., Wright, S.F. and Lovelock, C.E. (2010) 'Sedimentation within and among mangrove forests along a gradient of geomorphological settings', *Estuarine, Coastal and Shelf Science*, 86(1), 21-30. <https://doi.org/10.1016/j.ecss.2009.10.013>.
- Agüera-Vega, F., Carvajal-Ramírez, F., Martínez-Carricondo, P., López, J.S-H., Mesas-Carrascosa, F.J., García-Ferrer, A. and Pérez-Porras, F.J. (2018) 'Reconstruction of extreme topography from UAV structure from motion photogrammetry', *Measurement* 121, 127–138. <https://doi.org/10.1016/j.measurement.2018.02.062>.
- Ahmadabadian, A. H., Robson, S., Boehm, J., Shortis, M., Wenzel, K. and Fritsch, D. (2013) 'A comparison of dense matching algorithms for scaled surface reconstruction using stereo camera rigs', *ISPRS Journal of Photogrammetry and Remote Sensing*, 78, 157-167. <https://doi.org/10.1016/j.isprsjprs.2013.01.015>.
- Ahmed, S.S., Hulme, K.F., Fountas, G., Eker, U., Benedyk, I.V., Still, S.E. and Anastasopoulos, P.C. (2020) 'The flying car—Challenges and strategies toward future adoption', *Frontiers in Built Environment*, 6, 106. <https://doi.org/10.3389/fbuil.2020.00106>.
- Alongi, D.M., (2002) 'Present state and future of the worlds mangrove forests', *Environmental Conservation*, 29(3), 331-349. <https://doi.org/10.1017/S0376892902000231>.

- Anders, N., Valente, J., Masselink, R. and Keesstra, S. (2019) 'Comparing Filtering Techniques for Removing Vegetation from UAV-Based Photogrammetric Point Clouds', *Drones*, 3(3), 61. <https://doi.org/10.3390/drones3030061>.
- Anders, N. S., Seijmonsbergen, A. C. and Bouten, W. (2013) 'Geomorphological change detection using object-based feature extraction from multi-temporal LiDAR data', *IEEE Geoscience and Remote Sensing Letters*, 10(6), 1587-1591. <https://doi.org/10.1109/LGRS.2013.2262317>.
- Argyridis, A. and Argialas, D.P. (2015) 'A Fuzzy Spatial Reasoner for Multi-Scale Geobia Ontologies', *Photogrammetric Engineering and Remote Sensing*, 81, 491-498. <https://doi.org/10.14358/PERS.81.6.491>.
- Arya, S., Mount, D. M., Netanyahu, N. S., Silverman, R. and Wu, A. Y. (1998) 'An optimal algorithm for approximate nearest neighbor searching fixed dimensions', *Journal of the ACM*, 45(6), 891-923. <https://doi.org/10.1145/293347.293348>.
- Aryastana, P., Ardantha, I. M. and Candrayana, K. W. (2018) 'Coastline change analysis and erosion prediction using satellite images', In *MATEC Web of Conferences* (Vol. 197, 13003).
- Aucan, J. and Ridd, P.V. (2000) 'Tidal asymmetry in creek surrounded by saltflats and mangroves with small swamp slopes', *Wetlands Ecology and Management*, 8, 223-231. <https://doi.org/10.1023/A:1008459814925>.
- Axelsson, P. (2000) 'DEM generation from laser scanner data using adaptive TIN models', *International Archive of Photogrammetry and Remote Sensing*, 33 (4), 110-117.
- Axelsson, P. (1999) 'Processing of laser scanner data—algorithms and applications', *ISPRS Journal of Photogrammetry and Remote Sensing*, 54, 138-147. [https://doi.org/10.1016/S0924-2716\(99\)00008-8](https://doi.org/10.1016/S0924-2716(99)00008-8).
- Azian, M. and Mubarak, H. (2012). 'Functions and values of mangroves. In Status of Mangroves in Peninsular Malaysia', Omar, M., Aziz, K., Shamsudin, I., Raja Barizian, R.S., Eds.; Forest Research Institute Malaysia: Kuala Lumpur, Malaysia, 2012, 12-25.
- Babault, J., Bonnet, S., Crave, A. and Van Den Driessche, J. (2004) 'Influence of piedmont sedimentation on erosion dynamics of an uplifting landscape: an experimental approach', *Geology*, 33, 301-304. <https://doi.org/10.1130/G21095.1>.

- Bailly, J.S. and Levavasseur, F. (2012) 'Potential of linear features detection in a Mediterranean landscape from 3D VHR optical data: application to terrace walls', In *Geoscience and Remote Sensing Symposium (IGARSS)*, 7110–7113.
- Balaguer-Puig, M., Marqués-Mateu, Á., Lerma, J.L. and Ibáñez-Asensio, S. (2018) 'Quantifying small-magnitude soil erosion: Geomorphic change detection at plot scale', *Land Degradation and Development*, 29(3), 825-834. <https://doi.org/10.1002/ldr.2826>.
- Bandemer, H., and S. Gottwald (1995) 'Fuzzy Sets, Fuzzy Logic, Fuzzy Methods', John Wiley, Chichester, 250.
- Bangen, S.G., Wheaton J.M., and Bouwes, N. (2014b) 'A methodological intercomparison of topographic survey techniques for characterizing wadeable streams and rivers', *Geomorphology*, 206, 343–361. <https://doi.org/10.1016/j.geomorph.2013.10.010>.
- Bao, T.Q. (2011) 'Effect of mangrove forest structures on wave attenuation in coastal Vietnam', *Oceanologia*, 53(3), 807-818. <https://doi.org/10.5697/oc.53-3.807>.
- Bay, H., Ess, A., Tuytelaars, T. and Van Gool, L. (2008) 'Speeded-up robust features (SURF)', *Computer vision and image understanding*, 110(3), 346-359. <https://doi.org/10.1016/j.cviu.2007.09.014>.
- Bemis, S. P., Micklethwaite, S., Turner, D., James, M. R., Akciz, S., Thiele, S. T. and Bangash, H. A. (2014) 'Ground-based and UAV-based photogrammetry: A multi-scale, high-resolution mapping tool for structural geology and paleoseismology', *Journal of Structural Geology*, 69, 163-178. <https://doi.org/10.1016/j.jsg.2014.10.007>.
- Benassi, F., Dall'Asta, E., Diotri, F., Forlani, G., Morra di Cella, U., Roncella, R. and Santise, M., (2017) 'Testing accuracy and repeatability of UAV blocks oriented with GNSS-supported aerial triangulation', *Remote Sensing*, 9(2), 172. <https://doi.org/10.3390/rs9020172>.
- Bentley, J. L. (1975) 'Multidimensional binary search trees used for associative searching', *Communications of the ACM*, 18(9), 509-517. <https://doi.org/10.1145/361002.361007>.
- Berger, C., Schulze, M., Rieke-Zapp, D., and Schlunegger, F. (2010) 'Rill development and soil erosion: a laboratory study of slope and rainfall intensity', *Earth Surface Processes and Landforms*, 35, 1456–1467. <https://doi.org/10.1002/esp.1989>.

- Bird, S., Hogan, D., and Schwab, J., (2010) 'Photogrammetric monitoring of small streams under a riparian forest canopy', *Earth Surface Processes and Landforms*, 35, 952–970. <https://doi.org/10.1002/esp.2001>.
- Blake, M. (2020). 'GCPs vs RTK vs PPK: When to Use What and Why'. Retrieved from <https://waypoint.sensefly.com/gcps-rtk-ppk-when-what-why/>.
- Bone, E., dan Bolkom, C. (2003). Unmanned aerial vehicles: Background and issues *for congress*. DTIC Document.
- Brasington, J., Langham, J. and Rumsby, B. (2003) 'Methodological sensitivity of morphometric estimates of coarse fluvial sediment transport', *Geomorphology*, 53, 299–316. [https://doi.org/10.1016/S0169-555X\(02\)00320-3](https://doi.org/10.1016/S0169-555X(02)00320-3).
- Brasington, J., Rumsby, B. T. and McVey, R. A. (2000) 'Monitoring and modelling morphological change in a braided gravel-bed river using high resolution GPS-based survey', *Earth Surface Processes and Landforms*, 25(9), 973-990. [https://doi.org/10.1002/1096-9837\(200008\)25:9%3C973::AID-ESP111%3E3.0.CO;2-Y](https://doi.org/10.1002/1096-9837(200008)25:9%3C973::AID-ESP111%3E3.0.CO;2-Y).
- Brasington, J. and Smart, R.M.A. (2003) 'Close range digital photogrammetric analysis of experimental drainage basin evolution', *Earth Surface Processes and Landforms*, 28, 231–247. <https://doi.org/10.1002/esp.480>.
- Brown, C.R. and Giles, D.K. (2018) 'Measurement of pesticide drift from unmanned aerial vehicle application to a vineyard', *Transactions of the ASABE*, 61(5), 1539-1546. doi: 10.13031/trans.12672,
- Ca, V.T. and Xuyen, N.D. (2008) 'Tsunami risk along Vietnamese coast', *Journal of Water Resources and Environmental Engineering*, 23, 24-33. <https://doi.org/10.1016/B978-0-12-800007-6.00014-9>.
- Cahoon, D.R. (2006) 'A review of major storm impacts on coastal wetland elevations', *Estuaries and Coasts*, 29(6), 889-898. <https://doi.org/10.1007/BF02798648>.
- Cahoon, D.R., Reed, D.J. and Day, J.W. (1995a) 'Estimating shallow subsidence in microtidal salt marshes of the southeastern United States - Kaye and Barghoorn revisited', *Marine Geology*, 128(1-2), 1-9. [https://doi.org/10.1016/0025-3227\(95\)00087-F](https://doi.org/10.1016/0025-3227(95)00087-F).
- Cahoon, D. and Lynch, J.C. (1997) 'Vertical accretion and shallow subsidence in a mangrove forest of southwestern Florida, U.S.A', *Mangroves and Salt Marshes*, 1, 173-186. <https://doi.org/10.1023/A:1009904816246>.

- Cahoon, D.R., Hensel, P., Rybczyk, J., McKee, K.L., Proffitt, C.E. and Perez, B.C. (2003b) 'Mass tree mortality leads to mangrove peat collapse at Bay Islands, Honduras after Hurricane Mitch', *Journal of Ecology*, 91(6), 1093-1105. <https://doi.org/10.1046/j.1365-2745.2003.00841.x>.
- Cahoon, D.R., Hensel, P.F., Spencer, T., Reed, D.J., McKee, K.L. and Saintilan, N. (2006) 'Coastal wetland vulnerability to relative sea-level rise: wetland elevation trends and process controls', In: *Wetlands and Natural Resource Management* (eds. Verhoeven, J.T.A., Beltman, B., Bobbink, R. and Whigham, D.F.) *Ecological Studies* 190. 271 – 292. Springer-Verlag, Berlin, Heidelberg.
- Calonder, M., Lepetit, V., Strecha, C. and Fua, P. (2010) 'Brief: Binary robust independent elementary features', In *European conference on computer vision*, 778-792.
- Candido, B. M. (2019). Use of ground and air-based photogrammetry for soil erosion assessment. Ph.D. Thesis. Lancaster University; 2019.
- Carbonneau, P. E., Lane, S. N. and Bergeron, N. E. (2003) 'Cost-effective non-metric close-range digital photogrammetry and its application to a study of coarse gravel river beds', *International journal of remote sensing*, 24(14), 2837-2854. <https://doi.org/10.1080/01431160110108364>.
- Casado, M. R., Gonzalez, R. B., Kriechbaumer, T., and Veal, A. (2015). 'Automated identification of river hydromorphological features using UAV high resolution aerial imagery'. *Sensors*, 15(11), 27969-27989. <https://doi.org/10.3390/s151127969>.
- Casella, E., Rovere, A., Pedroncini, A., Mucerino, L., Casella, M., Cusati, L.A., Vacchi, M., Ferrari, M. and Firpo, M. (2014) 'Study of wave runup using numerical models and low-altitude aerial photogrammetry: A tool for coastal management', *Estuarine, Coastal and Shelf Science*, 149, 160-167. <https://doi.org/10.1016/j.ecss.2014.08.012>.
- Castillo, C., Pérez, R., James, M.R., Quinton, J.N., Taguas, E.V. and Gómez, J.A. (2012) 'Comparing the accuracy of several field methods for measuring gully erosion', *Soil Science Society of America Journal*, 76, 1319–1332. <https://doi.org/10.2136/sssaj2011.0390>.
- Cazenave, A., Lombard, A.T. and Llovel, W. (2008) 'Present-day sea level rise: A synthesis', *Comptes Rendus Geoscience*, 340, 761-770. <https://doi.org/10.1016/j.crte.2008.07.008>.

- Chakrastitha. (2015) ‘Drones – Unmanned Aerial Vehicles (UAVs), Types, Components, Works’. Retrieved from <https://electricalfundablog.com/drones-unmanned-aerial-vehicles-uavs/>.
- Chandler, J., Ashmore, P., Paola, C., Gooch, M. and Varkaris, F. (2002) ‘Monitoring river-channel change using terrestrial oblique digital imagery and automated digital photogrammetry’, *Annals of the Association of American Geographers*, 92(4), 631–644. <https://doi.org/10.1111/1467-8306.00308>.
- Chapman, A. (2016). ‘Types of Drones: Multi-Rotor vs Fixed-Wing vs Single Rotor vs Hybrid VTOL’. Retrieved from <https://www.cuav.com.au/articles/drone-types/>.
- Chen, S., Nikolaidis, E., Cudney, H., Rosca, R. and Haftka, R. (1999) ‘Comparison of probabilistic and fuzzy set methods for designing under uncertainty’. In *40th Structures, Structural Dynamics, and Materials Conference and Exhibit* (1579).
- Chen, Q., Gong, P., Baldocchi, D. and Xie, G. (2007) ‘Filtering airborne laser scanning data with morphological methods’, *Photogrammetric Engineering and Remote Sensing*, 73(2), 175–185. <https://doi.org/10.14358/PERS.73.2.175>.
- Chen, L., Ren, C., Zhang, B., Wang, Z. and Wang, Y. (2019) ‘Mapping spatial variations of structure and function parameters for forest condition assessment of the Changbai Mountain National Nature Reserve’, *Remote Sensing*, 11(24), 3004. <https://doi.org/10.3390/rs11243004>.
- Cintron, G. and Y.S. Novelli (1984) ‘Methods for studying mangrove structure. In, The Mangrove Ecosystem: Research Methods (eds. S.C. Snedaker and J.G. Snedaker)’, UNESCO, 91–113.
- Colomina, I. and Molina, P. (2014) ‘Unmanned aerial systems for photogrammetry and remote sensing: A review’, *ISPRS Journal of photogrammetry and remote sensing*, 92, 79-97. <https://doi.org/10.1016/j.isprsjprs.2014.02.013>.
- Congalton, R. G. and Green, K. (2009) ‘Assessing the accuracy of remotely sensed data: principles and practices’, 2nd ed. Boca Raton, FL: CRC Press/Taylor and Francis.
- Cook, K. L. (2017) ‘An evaluation of the effectiveness of low-cost UAVs and structure from motion for geomorphic change detection’, *Geomorphology*, 278, 195-208. <https://doi.org/10.1016/j.geomorph.2016.11.009>.

- Coveney, S. and Roberts, K., (2017) 'Lightweight UAV digital elevation models and orthoimagery for environmental applications: data accuracy evaluation and potential for river flood risk modelling', *International journal of remote sensing*, 38(8-10), 3159-3180.
<https://doi.org/10.1080/01431161.2017.1292074>.
- Dahdouh-Guebas F. (Ed.) (2020). World Mangroves database. Accessed at <http://www.vliz.be/vmdcdata/mangroves> on 2020-07-15.
- Dahdouh-Guebas, F. and N. Koedam, (2008) 'Long-term retrospection on mangrove development using transdisciplinary approaches: a review', *Aquatic Botany* 89(2), 80-92.
<https://www.sciencedirect.com/user/institution/login?targetUrl=%2Fscience%2Farticle%2Fpii%2FS0304377008000508>.
- Da Jiang Innovations (DJI). DJI Phantom 4. Available online: <https://www.dji.com/phantom-4/info> (accessed on 26 August 2019).
- Dandois, J. P. and Ellis, E. C. (2010) 'Remote sensing of vegetation structure using computer vision', *Remote sensing*, 2(4), 1157-1176.
<https://doi.org/10.3390/rs2041157>.
- de Haas, T., Ventra, D., Carbonneau, P. E. and Kleinhans, M. G. (2014) 'Debris-flow dominance of alluvial fans masked by runoff reworking and weathering', *Geomorphology*, 217, 165-181.
<https://www.sciencedirect.com/science/journal/0169555X/217/supp/C>.
- Dela-Cruz, M.J. and Koohafkan, P. (2009) 'Globally important agricultural heritage systems: a shared vision of agricultural, ecological and traditional societal sustainability', *Resources Science*, 31(6), 905–913.
- DeLong, S.B., Prentice, C.S., Hilley, G.E. and Ebert, Y. (2012) 'Multitemporal ALSM change detection, sediment delivery, and process mapping at an active earthflow', *Earth Surface Processes and Landforms*, 37(3), 262-272.
<https://doi.org/10.1002/esp.2234>.
- Deltares. (2014). Habitat requirements for mangroves. Available at: <https://publicwiki.deltares.nl/display/BWN/Building+Block+Habitat+requirements+for+mangroves>.
- Department of Surveying and Mapping Malaysia (DSMM). Malaysian Geoid Model (MyGEOID) Guidelines; Department of Surveying and Mapping Malaysia (DSMM): Kuala Lumpur, Malaysia, 2005.

- Detert, M. and Weitbrecht, V. (2012, September). Automatic object detection to analyze the geometry of gravel grains—a free stand-alone tool. In *River flow* (595-600). Taylor and Francis Group London.
- Detert, M. and Weitbrecht, V. (2013) ‘User guide to gravelometric image analysis by BASEGRAIN’, *Advances in Science and Research; Fukuoka, S., Nakagawa, H., Sumi, T., Zhang, H., Eds*, 1789-1795.
- Dietrich, J. T. (2016) ‘Riverscape mapping with helicopter-based Structure-from-Motion photogrammetry’, *Geomorphology*, 252, 144-157. <https://doi.org/10.1016/j.geomorph.2015.05.008>.
- Din, A.H.M., Zulkifli, N.A., Hamden, M.H. and Aris, W.A.W. (2019) ‘Sea level trend over Malaysian seas from multi-mission satellite altimetry and vertical land motion corrected tidal data’, *Advances in Space Research*, 63, 11, 3452-3472. <http://dx.doi.org/10.1016/j.asr.2019.02.022>.
- Donato, D. C., Kauffman, J. B., Murdiyarso, D., Kurnianto, S., Stidham, M. and Kanninen, M. (2011) ‘Mangroves among the most carbon-rich forests in the tropics’, *Nature Geoscience*, 4(5), 293–297. <https://doi.org/10.1038/ngeo1123>.
- Duró, G., Crosato, A., Kleinhans, M. G., and Uijttewaal, W. S. (2018) ‘Bank erosion processes measured with UAV-SfM along complex banklines of a straight mid-sized river reach’, *Earth Surface Dynamics*, 6(4), 933. <https://doi.org/10.5194/esurf-6-933-2018>.
- Duke, N.C., (2006) ‘Australia's mangroves’. University of Queensland, Brisbane, Australia, 200.
- Duke, N.C., J.-O. Meynecke, S. Dittmann, A.M. Ellison, K. Anger, U. Berger, S. Cannicci, K. Diele, K.C. Ewel, C.D. Field, N. Koedam, S.Y. Lee, C. Marchand, I. Nordhaus and F. Dahdouh-Guebas, (2007) ‘A world without mangroves?’ *Science* 317, 41-42. <https://doi.org/10.1126/science.317.5834.41b>.
- Dyer, K.R. (1973) ‘Estuaries: A Physical Introduction’. John Wiley and Sons, London, 140.
- D'Oleire-Oltmanns, S., Marzloff, I., Peter, K. D. and Ries, J. B. (2012) ‘Unmanned aerial vehicle (UAV) for monitoring soil erosion in Morocco’, *Remote Sensing*, 4(11), 3390-3416. <https://doi.org/10.3390/rs4113390>.
- Eisenbeiss, H. (2004) ‘A mini unmanned aerial vehicle (UAV): system overview and image acquisition’, *International Archives of Photogrammetry. Remote Sensing and Spatial Information Sciences*, 36(5/W1).

- Ekaso, D., Nex, F. and Kerle, N. (2020) 'Accuracy assessment of real-time kinematics (RTK) measurements on unmanned aerial vehicles (UAV) for direct georeferencing', *Geo-spatial information science*, 23(2), 165-181. <https://doi.org/10.1080/10095020.2019.1710437>.
- Elkhrachy, I. (2018) 'Vertical accuracy assessment for SRTM and ASTER Digital Elevation Models: A case study of Najran city, Saudi Arabia', *Ain Shams Engineering Journal*, 9(4), 1807-1817. <https://doi.org/10.1016/j.asej.2017.01.007>.
- Ellison, J.C. (2008) 'Long-term retrospection on mangrove development using sediment cores and pollen analysis: a review', *Aquatic Botany*, 89(2), 93-104. <https://doi.org/10.1016/j.aquabot.2008.02.007>.
- Elmqvist, M., Jungert, E., Lantz, F., Persson, Å. and Söderman, U. (2001) 'Terrain modelling and analysis using laser scanning data', *International Archives of Photogrammetry, Remote Sensing and Spatial Information Sciences*, 34, 219–226.
- Eltner, A., Baumgart, P., Maas, H. G. and Faust, D. (2015) 'Multi-temporal UAV data for automatic measurement of rill and interrill erosion on loss soil', *Earth Surface Processes and Landforms*, 40(6), 741-755. <https://doi.org/10.1002/esp.3673>.
- Eltner, A., Maas, H-G. and Faust, D. (2018) 'Soil micro-topography change detection at hillslopes in fragile Mediterranean landscapes', *Geoderma* 313, 217–232. <https://doi.org/10.1016/j.geoderma.2017.10.034>.
- ESSA, (2019). Geomorphic Change Detection (GCD). Access from <https://essa.com/explore-essa/tools/geomorphic-change-detection>.
- Evans, J.S. and Hudak, A.T. (2007) 'A multiscale curvature algorithm for classifying discrete return LiDAR in forested environments', *IEEE Transaction of Geoscience and Remote Sensing*, 45(4), 1029-1038. <https://doi.org/10.1109/TGRS.2006.890412>.
- Faiçal, B.S., Costa, F.G., Pessin, G., Ueyama, J., Freitas, H., Colombo, A., Fini, P.H., Villas, L., Osório, F.S., Vargas, P.A. and Braun, T. (2014) 'The use of unmanned aerial vehicles and wireless sensor networks for spraying pesticides'. *Journal of Systems Architecture*, 60(4), 393-404. <https://doi.org/10.1016/j.sysarc.2014.01.004>.

- Faiçal, B.S., Freitas, H., Gomes, P.H., Mano, L.Y., Pessin, G., de Carvalho, A.C., Krishnamachari, B. and Ueyama, J. (2017) 'An adaptive approach for UAV-based pesticide spraying in dynamic environments', *Computers and Electronics in Agriculture*, 138, 210-223. <https://doi.org/10.1016/j.compag.2017.04.011>.
- Farnsworth, E.J. and A.M. Ellison, (1997) 'Global conservation status of mangroves', *Ambio*, 26(6), 328-334.
- Favalli, M., Fornaciai, A., Isola, I., Tarquini, S. and Nannipieri, L. (2012) 'Multiview 3D reconstruction in geosciences', *Computers and Geosciences*, 44, 168-176. <https://doi.org/10.1016/j.cageo.2011.09.012>.
- Fazeli, H., Samadzadegan, F. and Dadrasjavan, F. (2016) 'Evaluating the potential of RTK-UAV for automatic point cloud generation in 3D rapid mapping', *The International Archives of Photogrammetry, Remote Sensing and Spatial Information Sciences*, 41, 221.
- Fengbo, Y., Xinyu, X., Ling, Z. and Zhu, S., (2017) 'Numerical simulation and experimental verification on downwash air flow of six-rotor agricultural unmanned aerial vehicle in hover', *International Journal of Agricultural and Biological Engineering*, 10(4), 41-53. <http://dx.doi.org/10.25165/j.ijabe.20171004.3077>.
- Fischler, M. A. and Bolles, R. C. (1981) 'Random sample consensus: a paradigm for model fitting with applications to image analysis and automated cartography', *Communications of the ACM*, 24(6), 381-395. <https://doi.org/10.1145/358669.358692>.
- Fisher, P. and Tate, N. (2006) 'Causes and consequences of error in digital elevation models', *Progress in Physical Geography*, 30(4), 467-489. <https://doi.org/10.1191/0309133306pp492ra>.
- Flener, C., Vaaja, M., Jaakkola, A., Krooks, A., Kaartinen, H., Kukko, A., Kasvi, E., Hyypä, H., Hyypä, J. and Alho, P. (2013) 'Seamless mapping of river channels at high resolution using mobile LiDAR and UAV-photography', *Remote Sensing*, 5(12), 6382-6407. <https://doi.org/10.3390/rs5126382>.
- Food and Agriculture (FAO) (2020). Global Forest Resources Assessment 2020: Main report. Rome. <https://doi.org/10.4060/ca9825en>
- Food and Agriculture Organization (FAO) (2007). The World's Mangrove 1980–2005. FAO Forestry Paper 153. FAO, Rome. 77.

- Food and Agriculture Organization (FAO) (2010). Global Forest Resources Assessment 2010. FAO Forestry Paper 163. FAO, Rome. 340.
- Forlani, G., Dall'Asta, E., Diotri, F., Cella, U.M.D., Roncella, R. and Santise, M. (2018) 'Quality assessment of DSMs produced from UAV flights georeferenced with on-board RTK positioning', *Remote Sensing*, 10(2), 311. <https://doi.org/10.3390/rs10020311>.
- Fonstad, M.A., Dietrich, J.T., Courville, B.C., Jensen, J.L. and Carbonneau, P.B. (2013) 'Topographic structure from motion: a new development in photogrammetric measurement', *Earth Surface Processes and Landforms*, 38, 421–430. <https://doi.org/10.1002/esp.3366>.
- Forkuor, G. and Maathuis, B. (2012) 'Comparison of SRTM and ASTER derived digital elevation models over two regions in Ghana-Implications for hydrological and environmental modeling', INTECH Open Access Publisher.
- Frankl, A., Stal, C., Abraha, A., Nyssen, J., Rieke-Zapp, D., De Wulf, A. and Poesen, J. (2015) 'Detailed recording of gully morphology in 3D through image-based modelling', *Catena*, 127, 92-101. <https://doi.org/10.1016/j.catena.2014.12.016>.
- Friedman, J. H., Bentley, J. L. and Finkel, R. A. (1977) 'An algorithm for finding best matches in logarithmic expected time', *ACM Transactions on Mathematical Software (TOMS)*, 3(3), 209-226. <https://doi.org/10.1145/355744.355745>.
- Fuller, I.C., Basher, L., Marden, M. and Massey, C. (2011) 'Using Morphological Adjustments to Appraise Sediment Flux', *Journal of Hydrology*, 50, 59-79. <https://search.informit.org/doi/10.3316/informit.315172004256339>.
- Fuller, I.C., Large, A.R.G, Charlton, M.E, Heritage, G.L. and Milan, D.J. (2003) 'Reach-scale sediment transfers: an evaluation of two morphological budgeting approaches', *Earth Surface Processes and Landforms*, 28, 889-903. <https://doi.org/10.1002/esp.1011>.
- Fuller, I.C., Richardson, J.M., Basher, L., Dykes, R.C. and Vale, S.S. (2012) 'Responses to river management? Geomorphic change over decadal and annual timescales in two gravel-bed rivers in New Zealand. In River Channels: Types', *Dynamics and Changes*, Molina D (ed). Nova Science: New York, 137-163.

- Furukawa, K. and E. Wolanski (1996) 'Sedimentation in mangrove forests', *Mangroves and Salt Marshes*, 1, 3–10. <https://doi.org/10.1023/A:1025973426404>.
- Furukawa, K., Wolanski, E. and Mueller, H. (1997) 'Currents and sediment transport in mangrove forests', *Estuarine, Coastal and Shelf Science*, 44(3), 301-310. <https://doi.org/10.1006/ecss.1996.0120>.
- Furukawa, Y. and Ponce, J. (2006) 'Carved visual hulls for image-based modeling', *International journal of computer vision*, 81(1), 53-67. https://doi.org/10.1007/11744023_44.
- Furukawa, Y., Curlless, B., Seitz, S. M. and Szeliski, R. (2010, June) 'Towards internet-scale multi-view stereo', In *2010 IEEE computer society conference on computer vision and pattern recognition* (1434-1441). IEEE.
- Furukawa, Y., and Ponce, J. (2010) 'Accurate, dense, and robust multiview stereopsis', *IEEE transactions on pattern analysis and machine intelligence*, 32(8), 1362-1376. <https://doi.org/10.1109/TPAMI.2009.161>.
- Gessesse, G.D., Fuchs, H., Mansberger, R., Klik, A., Rieke-Zapp, D.H. (2010). 'Assessment of erosion, deposition and rill development on irregular soil surfaces using close range digital photogrammetry', *Photogrammetric Record*, 25, 299–318. <https://doi.org/10.1111/j.1477-9730.2010.00588.x>.
- Gesch, D. B., Oimoen, M. J., and Evans, G. A. (2014) 'Accuracy assessment of the US Geological Survey National Elevation Dataset, and comparison with other large-area elevation datasets: SRTM and ASTER' (Vol. 1008). US Department of the Interior, US Geological Survey.
- Ghanavati, E., Firouzabadi, P. Z., Jangi, A. A. and Khosravi, S. (2008) 'Monitoring geomorphologic changes using Landsat TM and ETM+ data in the Hendijan River delta, southwest Iran', *International journal of remote sensing*, 29(4), 945-959. <https://doi.org/10.1080/01431160701294679>.
- Giri, C., Pengra, B., Zhu, Z., Singh, A. and Tieszen L. (2007) 'Monitoring mangrove forest dynamics of the Sundarbans in Bangladesh and India using multitemporal satellite data from 1973–2000', *Estuarine, Coastal and Shelf Science*, 73, 91–100. <https://doi.org/10.1016/j.ecss.2006.12.019>.
- Gienko, G. A., and Terry, J. P. (2014) 'Three-dimensional modeling of coastal boulders using multi-view image measurements', *Earth surface processes and Landforms*, 39(7)', 853-864. <https://doi.org/10.1002/esp.3485>.

- GISGeography (2022) 'DEM, DSM & DTM Differences – A Look at Elevation Models in GIS', Access from <https://gisgeography.com/dem-dsm-dtm-differences/>.
- Glendell, M., McShane, G., Farrow, L., James, M., Quinton, J., Anderson, K., Evans, M., Benaud, P., Rawlins, B., Morgan, D., Jones, L., Kirkham, M., DeBell, L., Quine, T., Lark, M., Rickson, J. and Brazier, R. (2017) 'Testing the utility of structure from motion photogrammetry reconstructions using small unmanned aerial vehicles and ground photography to estimate the extent of upland soil erosion', *Earth Surface Processes and Landforms*, 42, 1860–1871. <https://doi.org/10.1002/esp.4142>.
- Goetz, J., Brenning, A., Marcer, M., Bodin, X., (2018) 'Modeling the precision of structure-from-motion multi-view stereo digital elevation models from repeated close-range aerial surveys', *Remote Sensing of Environment*, 210, 208–216. <http://dx.doi.org/10.1016/j.rse.2018.03.013>.
- Gómez-Gutiérrez A, Schnabel S, Berenguer-Sempere F, Lavado-Contador F, and Rubio-Delgado J., (2014) 'Using 3D photo-reconstruction methods to estimate gully headcut erosion', *Catena* 120, 91–101. <https://doi.org/10.1016/j.catena.2014.04.004>.
- Graham, R., and Koh, A., (2002) 'Digital Aerial Survey: Theory and Practice, CRC Press.
- Gruszczyński, W., Matwój, W. and Cwiąkała, P. (2017) 'Comparison of low-altitude UAV photogrammetry with terrestrial laser scanning as data-source methods for terrain covered in low vegetation', *ISPRS Journal of Photogrammetry and Remote Sensing*, 126, 168-179. <http://dx.doi.org/10.1016/j.isprsjprs.2017.02.015>.
- Gruszczyński, W., Puniach, E., Cwiąkała, P. and Matwój, W. (2019) 'Application of convolutional neural networks for low vegetation filtering from data acquired by UAVs'. *ISPRS Journal of Photogrammetry and Remote Sensing*, 158, 1-10. <https://www.sciencedirect.com/science/journal/09242716/158/supp/C>.
- Guimarães, U. S., Rodrigues, T. W. P., Galo, M. D. L. B. T. and Pamplona, V. M. S. (2014, July). 'Change detection applied on shorelines in the mouth of Amazon River'. In *2014 IEEE Geoscience and Remote Sensing Symposium* (2146-2149). IEEE.

- Guo, M., Shi, H., Zhao, J., Liu, P., Welbourne, D. and Lin, Q. (2016) 'Digital close range photogrammetry for the study of rill development at flume scale', *Catena* 143, 265–274. <https://doi.org/10.1016/j.catena.2016.03.036>.
- Gupta, S.G., Ghonge, D. and Jawandhiya, P.M. (2013) 'Review of unmanned aircraft system (UAS)', *International Journal of Advanced Research in Computer Engineering and Technology (IJARCET)*, 2.
- Gurnell, A.M. (1997) 'Channel change on the River Dee meanders, 1946–1992, from the analysis of air photographs', *Research and Management*, 13,13-26. [https://doi.org/10.1002/\(SICI\)1099-1646\(199701\)13:1%3C13::AID-RRR420%3E3.0.CO;2-W](https://doi.org/10.1002/(SICI)1099-1646(199701)13:1%3C13::AID-RRR420%3E3.0.CO;2-W).
- Halim, M.K.A (2019) 'Pemantauan Status dan Perubahan Bakau di Kilim, Langkawi Menggunakan Teknologi Penderiaan Jauh dan Sistem Maklumat Geografi'. (Master Thesis, Universiti Teknologi Malaysia).
- Hamid, A.I.A., Din, A.H.M., Hwang, C., Khalid, N.F., Tugi, A. and Omar, K.M. (2018) 'Contemporary sea level rise rates around Malaysia: Altimeter data optimization for assessing coastal impact', *Journal of Asian Earth Sciences*, 166, 247-259. <http://dx.doi.org/10.1016/j.jseaes.2018.07.034>.
- Hamshaw, S. D., Bryce, T., O'Neil Dunne, J., Rizzo, D. M., Frolik, J., Engel, T. and Dewoolkar, M. M. (2017) 'Quantifying streambank erosion using unmanned aerial systems at site-specific and river network scales' *Geotechnical Frontiers*, 499-508. <http://dx.doi.org/10.1061/9780784480458.051>.
- Hamshaw, S. D., Engel, T., Rizzo, D. M., O'Neil-Dunne, J. and Dewoolkar, M. M. (2019) 'Application of unmanned aircraft system (UAS) for monitoring bank erosion along river corridors', *Geomatics, Natural Hazards and Risk*, 10(1), 1285-1305. <https://doi.org/10.1080/19475705.2019.1571533>.
- Hang, H.T.M., K. Hirose, D.V. Quy, T. Triet, N.H. Anh, Y. Maruyama and Y. Shiokawa (2003) 'Geo-environmental research for Can Gio mangrove forest, Vietnam', *Asian Journal of Geoinformatics*, 3, 3-11.
- Hänsel, P., Schindewolf, M., Eltner, A., Kaiser, A. and Schmidt, J. (2016) 'Feasibility of high- resolution soil erosion measurements by means of rainfall simulations and SfM photogrammetry', *Hydrology*, 3(38). <https://doi.org/10.3390/hydrology3040038>.

- Hanson, G.J. and Cook, K.R. (2004) 'Apparatus, test procedures, and analytical methods to measure soil erodibility in situ', *Applied Engineering in Agriculture* 20(4), 455-462. <http://dx.doi.org/10.13031/2013.16492>.
- Harwin, S., and Lucieer, A. (2012) 'Assessing the accuracy of georeferenced point clouds produced via multi-view stereopsis from unmanned aerial vehicle (UAV) imagery', *Remote Sensing*, 4(6), 1573-1599. <https://doi.org/10.3390/rs4061573>.
- He, X., (2018). 'Rapid development of unmanned aerial vehicles (UAV) for plant protection and application technology in China', *Outlooks on Pest Management*, 29(4), 162-167. http://dx.doi.org/10.1564/v29_aug_04.
- Heng, B.C.P., Chandler, J.H., and Armstrong, A., (2010) 'Applying close-range digital photogrammetry and soil erosion studies', *The Photogrammetric Record*, 25, 240–265. <https://doi.org/10.1111/j.1477-9730.2010.00584.x>.
- Hemmelder, S., Marra, W., Markies, H. and De Jong, S. M. (2018) 'Monitoring river morphology and bank erosion using UAV imagery—A case study of the river Büech, Hautes-Alpes, France', *International Journal of Applied Earth Observation and Geoinformation*, 73, 428-437. <https://doi.org/10.1016/j.jag.2018.07.016>.
- Heritage, G.L., Milan, D.J., Large, A.R.G. and Fuller, I.C. (2009) 'Influence of survey strategy and interpolation model on DEM quality', *Geomorphology*, 112, 334-344. <http://dx.doi.org/10.1016/j.geomorph.2009.06.024>.
- Hirt, C., Filmer, M. S. and Featherstone, W. E. (2010) 'Comparison and validation of the recent freely available ASTER-GDEM ver1, SRTM ver4. 1 and GEODATA DEM-9S ver3 digital elevation models over Australia', *Australian Journal of Earth Sciences*, 57(3), 337-347. <https://doi.org/10.1080/08120091003677553>.
- Hoff, R. Z., and Michel, J. J. M. (2014). Oil spills in mangroves: planning and response considerations.
- Hogarth P, J., (1999) 'The biology of mangroves', Oxford University Press, 228.
- Hong, P.N. and H.T. San (1993) 'Mangroves of Vietnam', The IUCN Wetlands Programme, IUCN, Bangkok, Thai, 173.
- Hong, P.N. (2006) 'The Role of Mangrove and Coral Reef Ecosystems in Natural Disaster Mitigation and Coastal Life Improvement', Agricultural Publishing House, Hanoi, 385.

- Hooke, J.M. and Yorke, L. (2011) 'Channel bar dynamics on multi-decadal timescales in an active meandering river', *Earth Surface Processes and Landforms*, 36. <https://doi.org/10.1002/esp.2214>.
- Hung, I., Unger, D., Kulhavy, D. and Zhang, Y. (2019) 'Positional precision analysis of orthomosaics derived from drone captured aerial imagery', *Drones*, 3(2), 46. <https://doi.org/10.3390/drones3020046>.
- Im, S.B., Hurlbaas, S. and Kang, Y.J. (2013) 'Summary review of GPS technology for structural health monitoring', *Journal of Structural Engineering*, 139(10), 1653-1664. [http://dx.doi.org/10.1061/\(ASCE\)ST.1943-541X.0000475](http://dx.doi.org/10.1061/(ASCE)ST.1943-541X.0000475).
- Immerzeel, W. W., Kraaijenbrink, P. D., Shea, J. M., Shrestha, A. B., Pellicciotti, F., Bierkens, M. F., and de Jong, S. M. (2014) 'High-resolution monitoring of Himalayan glacier dynamics using unmanned aerial vehicles', *Remote Sensing of Environment*, 150, 93-103. <http://dx.doi.org/10.1016/j.rse.2014.04.025>.
- International Civil Aviation Organization (ICAO). (2011) 'ICAO's circular 328 AN/190: Unmanned Aircraft Systems', Retrieved from http://www.icao.int/Meetings/UAS/Documents/Circular%20328_en.pdf
- International Union for Conservation of Nature (IUCN) (2020) 'Mangroves and coastal ecosystems', Retrieved from <http://www.iucn.org/theme/marine-and-polar/our-work/climate-change-and-ocean/mangroves-and-coastal-ecosystems>.
- Ismail, M.K.; Din, A.H. M; Uti, M.N.; Omar, A.H. Establishment of New Fitted Geoid Model in Universiti Teknologi Malaysia. In the International Archives of the Photogrammetry, Remote Sensing and Spatial Information. Sciences, Proceedings of the International Conference on Geomatics and Geospatial Technology (GGT 2018), Kuala Lumpur, Malaysia, 3–5 September 2018; ISPRS Archives: Hamburg, Germany, 2018; Volume XLII-4/W9.
- James, L.A, Hodgson, M.E, Ghoshal, S. and Latiolais, M.M. (2012) 'Geomorphic change detection using historic maps and DEM differencing: The temporal dimension of geospatial analysis', *Geomorphology*, 137, 181-198. <http://dx.doi.org/10.1016/j.geomorph.2010.10.039>.
- James, M.R. and Quinton, J.N. (2014) 'Ultra-rapid topographic surveying for complex environments: the hand-held mobile laser scanner (HMLS)', *Earth Surface. Processes and Landforms*, 39, 138–142. <https://doi.org/10.1002/esp.3489>.

- James, M. R. and Robson, S. (2012) 'Straightforward reconstruction of 3D surfaces and topography with a camera: Accuracy and geoscience application', *Journal of Geophysical Research: Earth Surface*, 117(F3). <https://doi.org/10.1029/2011JF002289>.
- James, M.R., Robson, S. and Smith, M.W. (2017) '3-D uncertainty-based topographic change detection with structure-from-motion photogrammetry: precision maps for ground control and directly georeferenced surveys', *Earth Surface Process Landforms*, 42, 1769-1788. <https://doi.org/10.1002/esp.4125>.
- James, M. R. and Varley, N. (2012) 'Identification of structural controls in an active lava dome with high resolution DEMs: Volcán de Colima, Mexico', *Geophysical Research Letters*, 39(22). <https://doi.org/10.1029/2012GL054245>.
- Jang, J. S. R., and Gulley, N. (2007). 'Fuzzy Logic Toolbox 2: User Guide, Matlab', Matlab, Natick, MA, 299. *Cerca con Google*.
- Jang, J. S. R., and Gulley, N. (2009). 'Fuzzy Logic Toolbox 2: User Guide, Matlab'. *Matlab, Natick, MA*.
- Januchowski, S.R., Pressey, R.L., VanDerWal, J. and Edwards, A. (2010) 'Characterizing errors in digital elevation models and estimating the financial costs of accuracy', *International Journal of Geographical Information Science* 24(9), 1327-1347. <https://doi.org/10.1080/13658811003591680>.
- Javernick, L., Brasington, J. and Caruso, B. (2014) 'Modelling the topography of shallowbraided rivers using Structure from Motion photogrammetry', *Geomorphology*, 213, 166–182. <https://doi.org/10.1016/j.geomorph.2014.01.006>.
- Javernick, L., Hicks, D. M., Measures, R., Caruso, B. and Brasington, J. (2016) 'Numerical modelling of braided rivers with structure-from-motion-derived terrain models', *River Research and Applications*, 32(5), 1071-1081. <http://dx.doi.org/10.1002/rra.2918>.
- Jayappa, K. S., Mitra, D. and Mishra, A. K. (2006) 'Coastal geomorphological and land-use and land-cover study of Sagar Island, Bay of Bengal (India) using remotely sensed data', *International Journal of Remote Sensing*, 27(17), 3671-3682. <https://doi.org/10.1080/01431160500500375>.
- Jayson-Quashigah, P. N., Addo, K. A. and Kodzo, K. S. (2013) 'Medium resolution satellite imagery as a tool for monitoring shoreline change', Case study of the

- Eastern coast of Ghana', *Journal of coastal Research*, (65), 511-516.
<http://dx.doi.org/10.2112/SI65-087.1>.
- John, D.M. and G.W. Lawson (1990) 'A review of mangrove and coastal ecosystems in West Africa and their possible relationships', *Estuarine, Coastal and Shelf Science*, 31, 505–518. [https://doi.org/10.1016/0272-7714\(90\)90009-G](https://doi.org/10.1016/0272-7714(90)90009-G).
- Jing, C., Shortridge, A., Lin, S., and Wu, J. (2014) 'Comparison and validation of SRTM and ASTER GDEM for a subtropical landscape in Southeastern China', *International Journal of Digital Earth*, 7(12), 969-992.
<https://doi.org/10.1080/17538947.2013.807307>.
- Jusoff, K. (2013) 'Malaysian Mangrove Forest and Their Significance to the Coastal Marine Environment', *Polish Journal of Environmental Studies*, 22(4), 979-1005.
- Kaiser, A., Neugirg, F., Rock, G., Müller, C., Haas, F., Ries, J. and Schmidt, J. (2014) 'Small-scale surface reconstruction and volume calculation of soil erosion in complex Moroccan gully morphology using structure from motion', *Remote Sensing*, 6(8), 7050-7080. <https://doi.org/10.3390/rs6087050>.
- Kaliraj, S., Chandrasekar, N. and Ramachandran, K. K. (2017) 'Mapping of coastal landforms and volumetric change analysis in the south west coast of Kanyakumari, South India using remote sensing and GIS techniques', *The Egyptian Journal of Remote Sensing and Space Science*, 20(2), 265-282.
<https://doi.org/10.1016/j.ejrs.2016.12.006>.
- Kanniah, K. D., Sheikhi, A., Cracknell, A. P., Goh, H. C., Tan, K. P., Ho, C. S. and Rasli, F. N. (2015) 'Satellite images for monitoring mangrove cover changes in a fast growing economic region in southern Peninsular Malaysia', *Remote Sensing*, 7(11), 14360-14385. <https://doi.org/10.3390/rs71114360>.
- Karleskint G. (1998) 'Introduction to marine biology', Harcourt Brace College Publishers. 378.
- Kathiresan, K. (2003) 'How do mangrove forests induce sedimentation?' *Revista De Biologia Tropical*, 51(2), 355-359.
- Keesstra, S., Nunes, J. P., Saco, P., Parsons, T., Poepl, R., Masselink, R. and Cerdà, A. (2018) 'The way forward: can connectivity be useful to design better measuring and modelling schemes for water and sediment dynamics?', *Science of the Total Environment*, 644, 1557-1572.
<https://doi.org/10.1016/j.scitotenv.2018.06.342>.

- Klir, G. J. and B. Yuan (1995) 'Fuzzy Sets and Fuzzy Logic: Theory and Applications', 592 pp. Prentice-Hall, Upper Saddle River, N. J.
- Kobashi, D. and Y. Mazda (2005) 'Tidal flow in riverine-type mangroves', *Wetlands Ecology and Management*, 13, 615– 619. <http://dx.doi.org/10.1007/s11273-004-3481-4>.
- Koparan, C., Koc, A. B., Privette, C. V. and Sawyer, C. B. (2018) 'In situ water quality measurements using an unmanned aerial vehicle (UAV) system', *Water*, 10(3), 264. <https://doi.org/10.3390/w10030264>.
- Koparan, C., Koc, A. B., Privette, C. V., Sawyer, C. B. and Sharp, J. L. (2018) 'Evaluation of a UAV-assisted autonomous water sampling', *Water*, 10(5), 655. <https://doi.org/10.3390/w10050655>.
- Koparan, C., Koc, A. B., Privette, C. V. and Sawyer, C. B. (2019) 'Autonomous in situ measurements of noncontaminant water quality indicators and sample collection with a UAV', *Water*, 11(3), 604. <https://doi.org/10.3390/w11030604>.
- Koparan, C., Koc, A. B., Privette, C. V. and Sawyer, C. B. (2020) 'Adaptive Water Sampling Device for Aerial Robots', *Drones*, 4(1), 5. <https://doi.org/10.3390/drones4010005>.
- Kraus, K. and Mikhail, E.M. (1972) 'Linear least squares interpolation', *Photogrammetric Engineering*, 38, 1016–1029
- Krauss, K.W., Allen, J.A. and Cahoon, D.R. (2003) 'Differential rates of vertical accretion and elevation change among aerial root types in Micronesian mangrove forests', *Estuarine, Coastal and Shelf Science*, 56(2), 251-259. [https://doi.org/10.1016/S0272-7714\(02\)00184-1](https://doi.org/10.1016/S0272-7714(02)00184-1).
- Krauss, K.W., Doyle, T.W., Doyle, T.J., Swarzenski, C.M., From, A.S., Day, R.H. and Conner, W.H. (2009) 'Water level observations in mangrove swamps during two hurricanes in Florida', *Wetlands* 29(1), 142-149. <https://doi.org/10.1672/07-232.1>.
- Krauss, K.W., McKee, K.L., Lovelock, C.E., Cahoon, D.R., Saintilan, N., Reef, R. and Chen, L. (2014) 'How mangrove forests adjust to rising sea level', *New Phytologist*, 202(1), 19-34. <https://doi.org/10.1111/nph.12605>.
- Kraus, K. and Pfeifer, N. (1998) 'Determination of terrain models in wooded areas with airborne laser scanner data', *ISPRS Journal of Photogrammetry and*

- Remote Sensing*, 53, 193–203. [https://doi.org/10.1016/S0924-2716\(98\)00009-4](https://doi.org/10.1016/S0924-2716(98)00009-4).
- Kuenzer, C., Bluemel, A., Gebhardt, S., Quoc, T.V. and Dech, S. (2011) ‘Remote sensing of mangrove ecosystems: A review’, *Remote Sensing*, 3, 878–928. <https://doi.org/10.3390/rs3050878>.
- Kuleli, T., Guneroglu, A., Karsli, F. and Dihkan, M. (2011) ‘Automatic detection of shoreline change on coastal Ramsar wetlands of Turkey’, *Ocean Engineering*, 38(10), 1141-1149. <http://dx.doi.org/10.1016/j.oceaneng.2011.05.006>.
- Kumara, M.P., Jayatissa, L.P., Krauss, K.W., Phillips, D.H. and Huxham, M. (2010) ‘High mangrove density enhances surface accretion, surface elevation change, and tree survival in coastal areas susceptible to sea-level rise’, *Oecologia*, 164(2), 545-553. <https://doi.org/10.1007/s00442-010-1705-2>.
- Kuwabara, R. (2002) ‘The role of the centroid in viviparous seeds of mangroves for transportation and dispersal’, *Mangrove Science*, 2, 29–35.
- Lane, S. N. (1998) ‘The use of digital terrain modelling in the understanding of dynamic river channel systems’, *Landform monitoring, modelling and analysis*, 311-342.
- Lane, S.N., (2000) ‘The measurement of river channel morphology using digital photogrammetry’, *The Photogrammetric Record* 16, 937–957. <https://doi.org/10.1111/0031-868X.00159>.
- Lane, S., Westaway, R. and Murray Hicks, D., (2003) ‘Estimation of erosion and deposition volumes in a large, gravel-bed, Braided River using synoptic remote sensing’, *Earth Surface Process Landform*, 28, 249–271. <https://doi.org/10.1002/esp.483>.
- Langran, G. (1992) *Time in Geographic Information Systems*. Taylor and Francis, London.
- Laporte-Fauret, Q., V. Marieu, B. Castelle, R. Michalet, S. Bujan, and D. Rosebery. (2019) ‘Low-cost UAV for high-resolution and large-scale coastal dune change monitoring using photogrammetry’, *Journal of Marine Science and Engineering*, 7, 63. <https://doi.org/10.3390/jmse7030063>.
- Lee, I.S. and Ge, L. (2006) ‘The performance of RTK-GPS for surveying under challenging environmental conditions’, *Earth, Planets and Space*, 58, 5, 515-522. <https://doi.org/10.1186/BF03351948>.

- Lee, J.O. and Sung, S.M. (2018) ‘Assessment of positioning accuracy of UAV photogrammetry based on RTK-GPS’, *Journal of the Korea Academia-Industrial cooperation Society*, 19, 4, 63-68. <https://doi.org/10.5762/KAIS.2018.19.4.63>.
- Le Hir, P., Monbet, Y. and Orvain, F. (2007) ‘Sediment erodability in sediment transport modelling: Can we account for biota effects?’ *Continental Shelf Research*, 27(8), 1116-1142. <http://dx.doi.org/10.1016/j.csr.2005.11.016>.
- Le Mauff, B., Juigner, M., Ba, A., Robin, M., Launeau, P. and Fattal, P. (2018) ‘Coastal monitoring solutions of the geomorphological response of beach-dune systems using multi-temporal LiDAR datasets (Vendée coast, France)’, *Geomorphology*, 304, 121-140. <http://dx.doi.org/10.1016/j.geomorph.2017.12.037>.
- Leon, J. X., Heuvelink, G. B. and S. R. Phinn (2014) ‘Incorporating DEM uncertainty in coastal inundation mapping’, *PLoS One*, 9(9). <https://doi.org/10.1371/journal.pone.0108727>.
- Leon, J. X., Roelfsema, C. M., Saunders, M. I. and Phinn, S. R. (2015) ‘Measuring coral reef terrain roughness using ‘Structure-from-Motion’ close-range photogrammetry’, *Geomorphology*, 242, 21-28. <http://dx.doi.org/10.1016/j.geomorph.2015.01.030>.
- Lermé, N. and Malgouyres, F. (2017) ‘A reduction method for graph cut optimization’, *Pattern Analysis and Applications*, 17, 361–378. <https://doi.org/10.1007/s10044-013-0337-7>.
- Li, Z. (1988) ‘On the measure of digital terrain model accuracy’, *The Photogrammetric Record*, 12(72), 873-877. <https://doi.org/10.1111/j.1477-9730.1988.tb00636.x>.
- Lhuillier, M. and Quan, L. (2005) ‘A quasi-dense approach to surface reconstruction from uncalibrated images’, *IEEE transactions on pattern analysis and machine intelligence*, 27(3), 418-433. <https://doi.org/10.1109/TPAMI.2005.44>.
- Li, J., Li, E., Chen, Y., Xu, L. and Zhang, Y. (2010, June) ‘Bundled depth-map merging for multi-view stereo’, In *2010 IEEE Computer Society Conference on Computer Vision and Pattern Recognition* (pp. 2769-2776). IEEE.
- Lisein, J., Linchant, J., Lejeune, P., Bouché, P. and Vermeulen, C. (2013) ‘Aerial surveys using an unmanned aerial system (UAS): comparison of different methods for estimating the surface area of sampling strips’, *Tropical*

- Conservation Science*, 6(4), 506-520.
<https://journals.sagepub.com/doi/10.1177/194008291300600405#translated-abstract-fr>.
- Liu, X. (2008) 'Airborne LiDAR for DEM generation: some critical issues', *Progress in Physical Geography*, 32, 31-49.
<https://doi.org/10.1177%2F0309133308089496>.
- Lo, C.F., Tsai, M.L., Chiang, K.W., Chu, C.H., Tsai, G.J., Cheng, C.K., El-Sheimy, N. and Ayman, H. (2015) 'The Direct Georeferencing Application and Performance Analysis of UAV Helicopter in GCP-Free Area'. *International Archives of the Photogrammetry, Remote Sensing and Spatial Information Sciences*, 40.
- Longuet-Higgins, H. C. (1981) 'A computer algorithm for reconstructing a scene from two projections', *Nature*, 293(5828), 133-135. <https://doi.org/10.1016/B978-0-08-051581-6.50012-X>.
- Lovelock, C.E., Bennion, V., Grinham, A. and Cahoon, D.R., (2011) 'The role of surface and subsurface processes in keeping pace with sea level rise in intertidal wetlands of Moreton Bay, Queensland, Australia', *Ecosystems*, 14(5), 745-757. <https://doi.org/10.1007/s10021-011-9443-9>.
- Lowe, D. G. (1999) 'Object recognition from local scale-invariant features', In *Proceedings of the seventh IEEE international conference on computer vision*, 2, 1150-1157.
- Lowe, D. G. (2001) 'Local feature view clustering for 3D object recognition', In *Proceedings of the 2001 IEEE Computer Society Conference on Computer Vision and Pattern Recognition. CVPR 2001 (Vol. 1, I-I)*.
- Lowe D.G. (2004) 'Distinctive image features from scale-invariant keypoints', *International Journal of Computer Vision*, 60, 91-110.
<https://doi.org/10.1023/B:VISI.0000029664.99615.94>.
- Lucieer, A., Jong, S.M.d. and Turner, D. (2014) 'Mapping landslide displacements using Structure from Motion (SfM) and image correlation of multi-temporal UAV photography', *Progress in Physical Geography*, 38, 97-116.
<https://doi.org/10.1177%2F0309133313515293>.

- Lugo, A.E. and S.C. Snedaker (1974) 'The ecology of mangroves', *Annual Review of Ecology and Systematics*, 5, 39–64. <https://doi.org/10.1146/annurev.es.05.110174.000351>.
- Maktav, D., Erbek, F. S. and Kabdasli, S. (2002) 'Monitoring coastal erosion at the Black Sea coasts in Turkey using satellite data: a case study at the Lake Terkos, north-west Istanbul', *International Journal of Remote Sensing*, 23(19), 4115-4124. <http://dx.doi.org/10.1080/01431160110115979>.
- Mancini, F., Dubbini, M., Gattelli, M., Stecchi, F., Fabbri, S. and Gabbianelli, G. (2013) 'Using unmanned aerial vehicles (UAV) for high-resolution reconstruction of topography: The structure from motion approach on coastal environments', *Remote sensing*, 5(12), 6880-6898. <https://doi.org/10.3390/rs5126880>.
- Marzolf, I. and Poesen, J. (2009) 'The potential of 3D gully monitoring with GIS using high resolution aerial photography and a digital photogrammetry system', *Geomorphology*, 111, 48–60. <http://dx.doi.org/10.1016/j.geomorph.2008.05.047>.
- Massel, S.R., K. Furukawa and R.M. Brinkman (1999) 'Surface wave propagation in mangrove forests', *Fluid Dynamics Research*, 24, 219–249. [https://doi.org/10.1016/S0169-5983\(98\)00024-0](https://doi.org/10.1016/S0169-5983(98)00024-0).
- Masselink, R. J., Heckmann, T., Temme, A. J., Anders, N. S., Gooren, H. P. and Keesstra, S. D. (2017) 'A network theory approach for a better understanding of overland flow connectivity', *Hydrological Processes*, 31(1), 207-220. <https://doi.org/10.1002/hyp.10993>.
- Mazda, Y. and Kamiyama, K. (2007) 'Tidal deformation and inundation characteristics within mangrove swamps', *Mangrove Science*, 4(5), 21-29.
- Mazda, Y., Yokochi, H. and Sato, Y (1990a) 'Groundwater flow in the Bashita-Minato mangrove area, and its influence on water and bottom mud properties', *Estuarine, Coastal and Shelf Science*, 31, 621–638. [https://doi.org/10.1016/0272-7714\(90\)90016-K](https://doi.org/10.1016/0272-7714(90)90016-K).
- Mazda, Y., Sato, Y, Sawamoto, S., Yokochi, H. and Wolanski, E. (1990b) 'Links between physical, chemical and biological processes in Bashita-Minato, a mangrove swamp in Japan', *Estuarine, Coastal and Shelf Science*, 31, 817–833. <https://doi.org/10.1016/0272-7714%2890%2990085-6>.

- Mazda, Y., Wolanski, E., King, B., Sase, A., Ohtsuka, D. and Magi, M. (1997) 'Drag force due to vegetation in mangrove swamps', *Mangroves and salt marshes*, 1(3), 193-199. <https://doi.org/10.1023/A:1009949411068>.
- Mazda, Y., Magi, M., Kogo, M. and Hong, P.N. (1997) 'Mangroves as a coastal protection from waves in the Tong King delta, Vietnam', *Mangroves and Salt marshes*, 1(2), 127-135. <https://doi.org/10.1023/A:1009928003700>.
- Mazda, Y., Kobashi, D. and Okada, S., (2005) 'Tidal-scale hydrodynamics within mangrove swamps', *Wetlands Ecology and Management*, 13(6), 647-655. <https://doi.org/10.1007/s11273-005-0613-4>.
- Mazda, Y., Magi, M., Ikeda, Y., Kurokawa, T. and Asano, T. (2006) 'Wave reduction in a mangrove forest dominated by *Sonneratia* sp.', *Wetlands Ecology and Management*, 14(4), 365-378. <http://dx.doi.org/10.1007/s11273-005-5388-0>.
- McIvor, A.L., Möller, I., Spencer, T. and Spalding, M. (2012a) 'Reduction of wind and swell waves by mangroves'. Natural Coastal Protection Series: Report 1. Cambridge Coastal Research Unit Working Paper 40. The Nature Conservancy and Wetlands International. 27 pp. URL: <http://www.coastalresilience.org/science/mangroves/reduction-wind-and-swell-waves-mangroves>.
- McIvor, A.L., Spencer, T., Möller, I. and Spalding, M. (2012b) 'Storm surge reduction by mangroves' Natural Coastal Protection Series: Report 2. Cambridge Coastal Research Unit Working Paper 41. The Nature Conservancy and Wetlands International. 35 pp. URL: <http://coastalresilience.org/science/mangroves/storm-surge-reduction-mangroves>
- McIvor, A.L., Spencer, T., Möller, I. and Spalding, M. (2013) 'The response of mangrove soil surface elevation to sea level rise', Natural Coastal Protection Series: Report 3. Cambridge Coastal Research Unit Working Paper 42. Published by The Nature Conservancy and Wetlands International. 59 pages. ISSN 2050-7941.
- McKee, K.L. and McGinnis, II, T.E. (2002) 'Hurricane Mitch: Effects on mangrove soil characteristics and root contributions to soil stabilization', USGS Open File Report 03-178, 57.
- McKee, K.L. and Vervaeke, W.C. (2009) 'Impacts of human disturbance on soil erosion potential and habitat stability of mangrove-dominated islands in the

- Pelican Cays and Twin Cays Ranges, Belize', *Smithsonian Contributions to the Marine Sciences*, 38, 415-427.
- McKee, K.L. (2011). 'Biophysical controls on accretion and elevation change in Caribbean mangrove ecosystems', *Estuarine, Coastal and Shelf Science*, 91(4), 475-483. <http://dx.doi.org/10.1016/j.ecss.2010.05.001>.
- Meesuk, V., Vojinovic, Z., Mynett, A. E. and Abdullah, A. F. (2015) 'Urban flood modelling combining top-view LiDAR data with ground-view SfM observations', *Advances in Water Resources*, 75, 105-117. <http://dx.doi.org/10.1016/j.advwatres.2014.11.008>.
- Meng, X., Shang, N., Zhang, X., Li, C., Zhao, K., Qiu, X. and Weeks, E. (2017) 'Photogrammetric UAV mapping of terrain under dense coastal vegetation: An object-oriented classification ensemble algorithm for classification and terrain correction', *Remote Sensing*, 9(11), 1187. <https://doi.org/10.3390/rs9111187>.
- Meng, X., Wang, L., Silván-Cárdenas, J.L. and Currit, N. (2009) 'A multi-directional ground filtering algorithm for airborne LIDAR', *ISPRS Journal of Photogrammetry and Remote Sensing*, 64, 117-124. <http://dx.doi.org/10.1016/j.isprsjprs.2008.09.001>.
- Mlambo, R., Woodhouse, I., Gerard, F. and Anderson, K. (2017) 'Structure from motion (SfM) Photogrammetry with drone data: a low cost method for monitoring greenhouse gas emissions from forests in developing countries', *Forests*, 8, 68. <https://doi.org/10.3390/f8030068>.
- Middleton, B.A. and McKee, K.L. (2001) 'Degradation of mangrove tissues and implications for peat formation in Belizean island forests', *Journal of Ecology*, 89, 818-828. <http://dx.doi.org/10.1046/j.0022-0477.2001.00602.x>.
- Milan, D.J., Heritage, G.L., Large, A.R.G. and Fuller, I.C. (2011) 'Filtering spatial error from DEMs: Implications for morphological change estimation', *Geomorphology*, 125, 160-171. <https://doi.org/10.1016/j.geomorph.2010.09.012>.
- Milne, J. A. and Sear, D. A. (1997) 'Modelling river channel topography using GIS', *International Journal of Geographical Information Science*, 11(5), 499-519. <https://doi.org/10.1080/136588197242275>.
- Mohamad, N., Khanan, M.F.A., Musliman, I.A., Kadir, W.H.W., Ahmad, A., Rahman, M.Z.A., Jamal, M.H., Zabidi, M., Suaib, N.M. and Zain, R.M. (2017) 'Riverbank erosion mapping using high resolution satellite image and

- unmanned aerial vehicle (UAV) approach', *In Proceeding of the 1st International Undergraduate and Postgraduate Students Conference on Marine Science, Technology and Management, Kuala Terenggamu*, 211-222.
- Mohamad, N., Khanan, M.F.A., Musliman, I.A., Kadir, W.H.W., Ahmad, A., Rahman, M.Z.A., Jamal, M.H., Zabidi, M., Suaib, N.M. and Zain, R.M. (2018) 'Spatio-temporal analysis of river morphological changes and erosion detection using very high resolution satellite image', *In IOP Conference Series: Earth and Environmental Science* (Vol. 169, No. 1, 012020). IOP Publishing.
- Mohamad, N. (2019) 'Evaluation of Riverbank Erosion Based on Mangrove Boundary Changes Identification Using Multi-Temporal Satellite Imagery', (Master Thesis, Universiti Teknologi Malaysia).
- Mohamad, N., Khanan, M. F. A., Ahmad, A., Din, M., Hassan, A. and Shahabi, H. (2019) 'Evaluating Water Level Changes at Different Tidal Phases Using UAV Photogrammetry and GNSS Vertical Data', *Sensors*, 19(17), 3778. <https://doi.org/10.3390/s19173778>.
- Mohamad, N., Ahmad, A., Khanan, M. F. A., and Din, A. H. M. (2022) 'Surface Elevation Changes Estimation underneath Mangrove Canopy Using SNERL Filtering Algorithm and DoD Technique on UAV-Derived DSM Data', *ISPRS International Journal of Geo-Information*, 11 (1), 32. <http://dx.doi.org/10.3390/ijgi11010032>
- Mohamad, N., Khanan, M.F.A., Ahmad, A. and Din, A.H.M (2020) 'Forecasting Future Riverbank Erosion Model Using Kernel Density and Line Buffering Method', *In Proceeding of 8th International Graduate Conference On Engineering, Science and Humanities (IGCESH 2020), Universiti Teknologi Malaysia, Johor, Malaysia*.
- Montealegre, A. L., Lamelas, M. T. and de la Riva, J. (2015) 'A comparison of open-source LiDAR filtering algorithms in a Mediterranean forest environment', *IEEE Journal of Selected Topics in Applied Earth Observations and Remote Sensing*, 8(8), 4072-4085. <http://dx.doi.org/10.1109/JSTARS.2015.2436974>.
- Morin, D., Planells, M., Guyon, D., Villard, L., Mermoz, S., Bouvet, A., Thevenon, H., Dejoux, J.F., Le Toan, T. and Dedieu, G. (2019) 'Estimation and mapping of forest structure parameters from open access satellite images: Development

- of a generic method with a study case on coniferous plantation’, *Remote Sensing*, 11(11), 1275. <https://doi.org/10.3390/rs11111275>.
- Morel, J. and Yu, G. (2009) ‘ASIFT: A new framework for fully affine invariant image comparison’, *Society for Industrial and Applied Mathematics Journal on Imaging Sciences*, 2, 438–469. <http://dx.doi.org/10.1137/080732730>.
- Mosbrucker, A.R., Major, J.J., Spicer, K.R. and Pitlick, J. (2017) ‘Camera system considerations for geomorphic applications of SfM photogrammetry’, *Earth Surface Processes and Landforms*, 42, 969–986. <https://doi.org/10.1002/esp.4066>.
- Mikolajczyk, K., Tuytelaars, T., Schmid, C., Zisserman, A., Matas, J., Schaffalitzky, F., Kadir, T. and Van Gool, L. (2005) ‘A comparison of affine region detectors’, *International journal of computer vision*, 65(1-2), 43-72. <https://doi.org/10.1007/s11263-005-3848-x>.
- Muja, M. and Lowe, D. G. (2009) ‘Fast approximate nearest neighbors with automatic algorithm configuration’, *VISAPP (1)*, 331-340. <https://doi.org/10.5220/0001787803310340>.
- Myers, D.T., Rediske, R.R. and McNair, J.N. (2019) ‘Measuring streambank erosion: A comparison of erosion pins, total station, and terrestrial laser scanner’, *Water*, 11, 9, 1846. <https://doi.org/10.3390/w11091846>.
- Nadal-Romero, E., Revuelto, J., Errea, P. and López-Moreno, J. I. (2015) ‘The application of terrestrial laser scanner and SfM photogrammetry in measuring erosion and deposition processes in two opposite slopes in a humid badlands area (central Spanish Pyrenees)’, *Soil*, 1(2), 561. <http://dx.doi.org/10.5194/soil-1-561-2015>.
- Nagai, M., Chen, T., Shibasaki, R., Kumagai, H. and Ahmed, A. (2009) ‘UAV-borne 3-D mapping system by multisensor integration’, *IEEE Transactions on Geoscience and Remote Sensing*, 47(3), 701-708. <http://dx.doi.org/10.1109/TGRS.2008.2010314>.
- Nagelkerken, I., Blaber, S.J.M., Bouillon, S., Green, P., Haywood, M., Kirton, L.G., Meynecke, J.O., Pawlik, J., Penrose, H.M., Sasekumar, A. and Somerfield, P.J. (2008) ‘The habitat function of mangroves for terrestrial and marine fauna: A review’, *Aquatic Botany* 89(2), 155-185. <http://dx.doi.org/10.1016/j.aquabot.2007.12.007>.

- Neugirg, F., Stark, M., Kaiser, A., Vlacilova, M., Della Seta, M., Vergari, F., Schmidt, J., Becht, M. and Haas, F. (2016) 'Erosion processes in calanchi in the Upper Orcia Valley, Southern Tuscany, Italy based on multitemporal high-resolution terrestrial LiDAR and UAV surveys', *Geomorphology*, 269, 8-22. <http://dx.doi.org/10.1016/j.geomorph.2016.06.027>.
- Neverman, A.J., Fuller, I.C. and Procter, J.N. (2016) 'Application of geomorphic change detection (GCD) to quantify morphological budgeting error in a New Zealand gravel-bed river: A case study from the Makaroro river, Hawke's bay', *Journal of Hydrology*, 45-63. <https://search.informit.org/doi/10.3316/informit.194414866333656>.
- Nex, F. and Remondino, F. (2014) 'UAV for 3D mapping applications: a review', *Applied geomatics*, 6(1), 1-15. <https://doi.org/10.1007/s12518-013-0120-x>.
- Nicosevici, T. and Garcia, R. (2008) 'Online robust 3D mapping using structure from motion cues', In *OCEANS 2008-MTS/IEEE Kobe Techno-Ocean, 2008*, IEEE, 1-7).
- Nikolakopoulos, K. G., Kamaratakis, E. K. and Chrysoulakis, N. (2006) 'SRTM vs ASTER elevation products. Comparison for two regions in Crete, Greece', *International Journal of remote sensing*, 27(21), 4819-4838. <https://doi.org/10.1080/01431160600835853>.
- Nouwakpo, S.K. and Huang, C.H., (2012) 'A simplified close-range photogrammetric technique for soil erosion assessment', *Soil Science Society of America Journal*, 76, 70–84. <http://dx.doi.org/10.2136/sssaj2011.0148>.
- Nouwakpo, S.K., James, M.R., Wetz, M.A., Huang, C.-H., Chagas and I., Lima, L. (2014) 'Evaluation of structure from motion for soil microtopography measurement', *The Photogrammetric Records*, 29, 297–316. <https://doi.org/10.1111/phor.12072>.
- Nunes, J.P., Wainwright, J., Biielders, C.L., Darboux, F., Fiener, P., Finger, D., and Turnbull, L. (2018) 'Better models are more effectively connected models', *Earth Surface Processes and Landforms*, 43, 1355–1360. <http://dx.doi.org/10.1002/esp.4323>.
- Ogura, K., Yamada, Y., Kajita, S., Yamaguchi, H., Higashino, T. and Takai M (2019) 'Ground object recognition and segmentation from aerial image-based 3D

- point cloud', *Computational Intelligence*, 35, 625–642.
<https://doi.org/10.1111/coin.12232>.
- Omar, H., Husin, T. M., H. and Parlan, I. (2020) 'Status of Mangroves in Malaysia', Forest Research Institute Malaysia, ISBN 978-967-2149-81-1.
- O'neal, M.A. and Pizzuto, J.E. (2011) 'The rates and spatial patterns of annual riverbank erosion revealed through terrestrial laser-scanner surveys of the South River, Virginia', *Earth Surface Processes and Landforms*, 36, 695-701.
<https://doi.org/10.1002/esp.2098>.
- Onrizal, A.G. and Mansor, M. (2017) 'Assessment of Natural Regeneration of Mangrove Species at Tsunami Affected Areas in Indonesia and Malaysia', *Proceeding of 1st Annual Applied Science and Engineering Conference*, 1- 6.
- Pagán, J.I., Bañon, L., López, I., Bañon, C. and Aragonés, L. (2019) 'Monitoring the dune-beach system of Guardamar del Segura (Spain) using UAV, SfM and GIS techniques', *Science of Total Environment*, 687, 1034–1045.
<http://dx.doi.org/10.1016/j.scitotenv.2019.06.186>.
- Palmer, J.A. (2008) 'An Assessment of Riparian Land-Use and Channel Condition Impacts on Streambank Eroding Lengths and Recession Rates in Two Third Order Rural Watersheds in Central Iowa'. (Master's Thesis, Iowa State University, Ames, IA, USA)
- Pandey, A., Himanshu, S. K., Mishra, S. K. and Singh, V. P. (2016) 'Physically based soil erosion and sediment yield models revisited', *Catena*, 147, 595-620.
<http://dx.doi.org/10.1016/j.catena.2016.08.002>.
- Peppas, M.V., Hall, J., Goodyear, J. and Mills, J.P. (2019) 'Photogrammetric assessment and comparison of DJI Phantom 4 pro and phantom 4 RTK small unmanned aircraft systems', *ISPRS Geospatial Week 2019*.
- Pfeifer, N., Stadler, P. and Briese, C. (2001) 'Derivation of digital terrain models in the SCOP++ environment', In Proceedings of OEEPE 1214 Workshop on Airborne Laser scanning and Interferometric SAR for Detailed Digital Terrain Models, Stockholm, Sweden, 2001, 1215-3612.
- Pijl, A., Bailly, J. S., Feurer, D., El Maaoui, M. A., Boussema, M. R. and Tarolli, P. (2020) 'TERRA: terrain extraction from elevation Rasters through repetitive anisotropic filtering', *International Journal of Applied Earth Observation and Geoinformation*, 84, 101977. <http://dx.doi.org/10.1016/j.jag.2019.101977>.

- Pijl, A., Barneveld, P., Mauri, L., Borsato, E., Grigolato, S. and Tarolli, P. (2019a) 'Impact of mechanisation on soil loss in terraced vineyard landscapes', *Cuadernos de Investigacion Geografica*, 45, 287–308. <http://dx.doi.org/10.18172/cig.3774>.
- Pijl, A., Tosoni, M., Roder, G., Sofia, G. and Tarolli, P. (2019b) 'Design of terrace drainage networks using UAV-based high-resolution topographic data', *Water*, 11(4), 814. <http://dx.doi.org/10.3390/w11040814>.
- Pinet P.R. (1998) 'Invitation to Oceanography', Jones and Barlett Publishers. 508.
- Polidoro, B.A., Carpenter, K.E., Collins, L., Duke, N.C., Ellison, A.M., Ellison, J.C., Farnsworth, E.J., Fernando, E.S., Kathiresan, K., Koedam, N.E. and Livingstone, S.R. (2010) 'The loss of species: mangrove extinction risk and geographic areas of global concern', *PLoS ONE*, 5(4), 10095. <https://doi.org/10.1371/journal.pone.0010095>.
- Ponti, M. P. (2012) 'Segmentation of low-cost remote sensing images combining vegetation indices and mean shift', *IEEE Geoscience and Remote Sensing Letters*, 10(1), 67-70. <http://dx.doi.org/10.1109/LGRS.2012.2193113>.
- Quartel, S., Kroon, A., Augustinus, P., Van Santen, P. and Tri, N.H. (2007) 'Wave attenuation in coastal mangroves in the Red River Delta, Vietnam', *Journal of Asian Earth Sciences*, 29(4), 576-584. <http://dx.doi.org/10.1016/j.jseaes.2006.05.008>.
- Ragia, L. and Krassakis, P. (2019) 'Monitoring the changes of the coastal areas using remote sensing data and geographic information systems', In *Seventh International Conference on Remote Sensing and Geoinformation of the Environment (RSCy2019)* (Vol. 11174, 111740X), International Society for Optics and Photonics.
- Rogers, K., Saintilan, N. and Cahoon, D., (2005) 'Surface elevation dynamics in a regenerating mangrove forest at Homebush Bay, Australia', *Wetlands Ecology and Management*, 13(5), 587-598. <https://doi.org/10.1007/s11273-004-0003-3>.
- Rogers, K., Wilton, K.M. and Saintilan, N. (2006) 'Vegetation change and surface elevation dynamics in estuarine wetlands of southeast Australia', *Estuarine, Coastal and Shelf Science*, 66(3-4), 559-569. <http://dx.doi.org/10.1016/j.ecss.2005.11.004>.

- Roggero, M. (2001) 'Airborne laser scanning: clustering in raw data', *International Archives of Photogrammetry Remote Sensing and Spatial Information Sciences*, 227–232.
- Ramírez-Cuesta, J. M., Rodríguez-Santalla, I., Gracia, F. J., Sánchez-García, M. J. and Barrio-Parra, F. (2016) 'Application of change detection techniques in geomorphological evolution of coastal areas. Example: Mouth of the River Ebro (period 1957–2013)', *Applied Geography*, 75, 12-27. <http://dx.doi.org/10.1016/j.apgeog.2016.07.015>.
- RAMSAR. (2003) 'Malaysia names three new Ramsar sites in Johor State'. Retrieved from <http://www.ramsar.org/news/malaysia-names-three-new-ramsar-sites-in-johor-state>.
- Remondino, F., Barazzetti, L., Nex, F., Scaioni, M. and Sarazzi, D. (2011) 'UAV photogrammetry for mapping and 3d modeling—current status and future perspectives', *International archives of the photogrammetry, remote sensing and spatial information sciences*, 38(1), C22.
- Rosnell, T. and Honkavaara, E. (2012) 'Point cloud generation from aerial image data acquired by a quadrocopter type micro unmanned aerial vehicle and a digital still camera', *Sensors*, 12(1), 453-480. <https://doi.org/10.3390/s120100453>.
- Ridd, P.V. and T. Stieglitz (2002) 'Dry season salinity changes in tropical mangrove and salt flat fringed estuaries', *Estuarine, Coastal and Shelf Science*, 54, 1039–1049. <http://dx.doi.org/10.1006/ecss.2001.0876>.
- Rieke-Zapp, D.H. and Nearing, M.A., (2005), 'Digital close range photogrammetry for measurement of soil erosion', *The Photogrammetric Records*, 20, 69–87. <http://dx.doi.org/10.1111/j.1477-9730.2005.00305.x>.
- Rippin, D. M., Pomfret, A. and King, N. (2015) 'High resolution mapping of supra-glacial drainage pathways reveals link between micro-channel drainage density, surface roughness and surface reflectance', *Earth Surface Processes and Landforms*, 40(10), 1279-1290. <https://doi.org/10.1002/esp.3719>.
- Rumsby, B.T, Brasington, J, Langham, J.A, Mclelland, S.J, Middleton, R. and Rollinson, G. (2008) 'Monitoring and modelling particle and reach-scale morphological change in gravel-bed rivers: Applications and challenges', *Geomorphology*, 93, 40-54. <http://dx.doi.org/10.1016/j.geomorph.2006.12.017>.

- Rumson, A.G., Hallett, S.H. and Brewer, T.R. (2019) 'The application of data innovations to geomorphological impact analyses in coastal areas: An East Anglia, UK, case study', *Ocean and Coastal Management*, 181, 104875. <http://dx.doi.org/10.1016/j.ocecoaman.2019.104875>.
- Ružić, I., Marović, I., Benac, Č. and Ilić, S. (2014) 'Coastal cliff geometry derived from structure-from-motion photogrammetry at Stara Baška, Krk Island, Croatia', *Geo-Marine Letters*, 34(6), 555-565. <https://doi.org/10.1007/s00367-014-0380-4>.
- Ryan, J.C., Hubbard, A.L., Box, J.E., Todd, J., Christoffersen, P., Carr, J.R., Holt, T.O. and Snooke, N. (2015) 'UAV photogrammetry and structure from motion to assess calving dynamics at Store Glacier, a large outlet draining the Greenland ice sheet', *The Cryosphere*, 9(1), 1-11. <http://dx.doi.org/10.5194/tc-9-1-2015>.
- Saad, S., Husain, M.L., Yaacob, R. and Asano, T. (1999) 'Sediment accretion and variability of sedimentological characteristics of a tropical estuarine mangrove: Kemaman, Terengganu, Malaysia', *Mangroves and Salt Marshes*, 3(1), 51-58. <http://dx.doi.org/10.1023/A:1009936014043>.
- Saenger, P. and Snedaker, S.C. (1993) 'Pantropical trends in mangrove above-ground biomass and annual litterfall', *Oecologia*, 96, 293-299. <https://doi.org/10.1007/BF00317496>.
- Sato, K. (2003) 'Reality of sedimentation in mangrove forest by the tide and discharge—Investigation on trapped amount of deposit in a serial of high tides—. A summary on the Mangrove Study in Okinawa (FY2000-2002)', Research Institute for Subtropics, 58–59.
- Seitz, S. M. and Dyer, C. R. (1999) 'Photorealistic scene reconstruction by voxel coloring', *International Journal of Computer Vision*, 35(2), 151-173. <https://doi.org/10.1023/A:1008176507526>.
- Seitz, S.M., Curless, B., Diebel, J., Scharstein, D. and Szeliski, R. (2006) 'A comparison and evaluation of multi-view stereo reconstruction algorithms'. *Computer Vision and Pattern Recognition, 2006 IEEE Computer Society Conference*, 519–528.
- Sesli, F. A., Karsli, F., Colkesen, I. and Akyol, N. (2009) 'Monitoring the changing position of coastlines using aerial and satellite image data: an example from the eastern coast of Trabzon, Turkey', *Environmental Monitoring and Assessment*, 153(1-4), 391-403. <https://doi.org/10.1007/s10661-008-0366-7>.

- Shahida, N., Majid, Z. and Setan, H., (2010) 'DTM generation from LiDAR data by using different filters in open-source software', *Geoinformation Science Journal*, 10 (2), 89-109.
- Shan, J. and Aparajithan, S. (2005) 'Urban DEM generation from raw Lidar data' *Photogrammetric Engineering and Remote Sensing*, 71, 217–226. <http://dx.doi.org/10.14358/PERS.71.2.217>.
- Shen, Y.L., Liu, J., Wu, L.X., Li, F.S. and Wang, Z. (2011) 'Reconstruction of disaster scene from UAV images and flight-control data', *Geography and Geo-Information Science*, 27(6), 13-17. <http://dx.10.1007/s11589-011-0776-4>.
- Siart, C., Bubenzer, O. and Eitel, B. (2009) 'Combining digital elevation data (SRTM/ASTER), high resolution satellite imagery (Quickbird) and GIS for geomorphological mapping: A multi-component case study on Mediterranean karst in Central Crete', *Geomorphology*, 112(1-2), 106-121. <http://dx.doi.org/10.1016/j.geomorph.2009.05.010>.
- Siebert, S. and Teizer, J. (2014) 'Mobile 3D mapping for surveying earthwork projects using an Unmanned Aerial Vehicle (UAV) system', *Automation in construction*, 41, 1-14. <http://dx.doi.org/10.1016/j.autcon.2014.01.004>.
- Sithole, G. (2001) 'Filtering of laser altimetry data using a slope adaptive filter. Int. Arch. Photogramm', *International Archives of Photogrammetry Remote Sensing and Spatial Information Sciences*, 203–210.
- Sithole, G. and Vosselman, G., (2004) 'Experimental comparison of filter algorithms for bare- Earth extraction from airborne laser scanning point clouds', *ISPRS Journal of Photogrammetry and Remote Sensing*, 59, 85–101. <http://dx.doi.org/10.1016/j.isprsjprs.2004.05.004>.
- Smith, M. W., Carrivick, J. L., Hooke, J. and Kirkby, M. J. (2014) 'Reconstructing flash flood magnitudes using 'Structure-from-Motion': A rapid assessment tool', *Journal of Hydrology*, 519, 1914-1927. <http://dx.doi.org/10.1016/j.jhydrol.2014.09.078>.
- Smith. M.W. and Vericat, D. (2015) 'From experimental plots to experimental landscapes: Topography, erosion and deposition in sub-humid badlands from Structure from Motion photogrammetry', *Earth Surface Processes and Landforms*, 4, 1656–1671. <http://dx.doi.org/10.1002/esp.3747>.

- Smith, M. W., Carrivick, J. L. and Quincey, D. J. (2016) 'Structure from motion photogrammetry in physical geography', *Progress in Physical Geography*, 40(2), 247-275. <http://dx.doi.org/10.1177/0309133315615805>.
- Snavely, N., Seitz, S. M. and Szeliski, R. (2008) 'Modeling the world from internet photo collections', *International journal of computer vision*, 80(2), 189-210. <http://dx.doi.org/10.1007/s11263-007-0107-3>.
- Snedaker, S.C. and Snedaker, J.G. (1984) 'The Mangrove Ecosystem: Research Methods', UNESCO, 251.
- Sofia, G., Bailly, J.S., Chehata, N., Tarolli, P. and Levavasseur, F. (2016) 'Comparison of pleiades and LiDAR digital elevation models for terraces detection in farmlands', *IEEE Journal of Selected Topics in Applied Earth Observations and Remote Sensing*, 9, 1567–1576. <http://dx.doi.org/10.1109/JSTARS.2016.2516900>.
- Sohn, G. and Dowman, I., (2002) 'Terrain surface reconstruction by the use of tetrahedron model with the MDL criterion', *International Archives of the Photogrammetry, Remote Sensing and Spatial Information Sciences*, XXXIV, 336–344.
- Spalding, M., Blasco, F. and Field, C. (1997) 'World Mangrove Atlas', The International Society for Mangrove Ecosystems, 178.
- Squires, J. R., DeCesare, N. J., Olson, L. E., Kolbe, J. A., Hebblewhite, M. and Parks, S. A. (2013) 'Combining resource selection and movement behavior to predict corridors for Canada lynx at their southern range periphery', *Biological Conservation*, 157, 187-195. <https://doi.org/10.1016/J.BIOCON.2012.07.018>.
- Stumpf, A., Malet, J. P., Allemand, P., Pierrot-Deseilligny, M. and Skupinski, G. (2015) 'Ground-based multi-view photogrammetry for the monitoring of landslide deformation and erosion', *Geomorphology*, 231, 130-145. <http://dx.doi.org/10.1016/j.geomorph.2014.10.039>.
- Strecha, C., Bronstein, A., Bronstein, M. and Fua, P. (2011) 'LDAHash: Improved matching with smaller descriptors', *IEEE transactions on pattern analysis and machine intelligence*, 34(1), 66-78. <http://dx.doi.org/10.1109/TPAMI.2011.103>.
- Štroner, M., Urban, R., Lidmila, M., Kolář, V., and Křemen, T. (2021) 'Vegetation Filtering of a Steep Rugged Terrain: The Performance of Standard Algorithms

- and a Newly Proposed Workflow on an Example of a Railway Ledge', *Remote Sensing*, 13(15), 3050. <https://doi.org/10.3390/rs13153050>.
- Suliman, A. and Zhang, Y. (2016) 'Segment-Based Terrain Filtering Technique for Elevation-Based Building Detection in VHR Remote Sensing Images', *Advances in Remote Sensing*, 5(3), 192-202. <http://dx.doi.org/10.4236/ars.2016.53016>.
- Surian, N. (1999) 'Channel changes due to river regulation: the case of the Piave River, Italy', *Earth Surface Processes and Landforms*, 24, 1135-1151. [https://doi.org/10.1002/\(SICI\)1096-9837\(199911\)24:12%3C1135::AID-ESP40%3E3.0.CO;2-F](https://doi.org/10.1002/(SICI)1096-9837(199911)24:12%3C1135::AID-ESP40%3E3.0.CO;2-F).
- Taddia, Y., Stecchi, F. and Pellegrinelli, A. (2020) 'Coastal Mapping using DJI Phantom 4 RTK in Post-Processing Kinematic Mode', *Drones*, 4(2), 9. <https://doi.org/10.3390/drones4020009>.
- Tamassoki, E., Amiri, H. and Soleymani, Z. (2014) 'Monitoring of shoreline changes using remote sensing (case study: coastal city of Bandar Abbas)', In *IOP conference series: earth and environmental science* (Vol. 20, No. 1, 012023). IOP Publishing.
- Tammaing, A. D., Eaton, B. C. and Hugenholtz, C. H. (2015) 'UAS-based remote sensing of fluvial change following an extreme flood event', *Earth Surface Processes and Landforms*, 40(11), 1464-1476. <http://dx.doi.org/10.1002/esp.3728>.
- Tan, Y., Wang, S., Xu, B. and Zhang, J. (2018) 'An improved progressive morphological filter for UAV-based photogrammetric point clouds in river bank monitoring', *ISPRS Journal of Photogrammetry and Remote Sensing*, 146, 421-429. <https://www.sciencedirect.com/science/journal/09242716>.
- Tarolli, P., Sofia, G., Calligaro, S., Prosdocimi, M., Preti, F. and Dalla Fontana, G. (2015) 'Vineyards in terraced landscapes: new opportunities from lidar data', *Land Degradation and Development*, 26, 92-102. <https://doi.org/10.1002/ldr.2311>.
- Taureau, F., Robin, M., Proisy, C., Fromard, F., Imbert, D. and Debaine, F. (2019) 'Mapping the mangrove forest canopy using spectral unmixing of very high spatial resolution satellite images', *Remote Sensing*, 11(3), 367. <https://doi.org/10.3390/rs11030367>.

- Taylor, J.R. (1997) 'An Introduction to Error Analysis: the Study of Uncertainties in Physical Measurements, second edition', University Science Books: Sausalito, California.
- The Editor of Encyclopedia Britannica, (2019) 'Mangrove', Encyclopedia Britannica, published on April 24 (2019), access on December 03, 2020, URL: <https://www.britannica.com/plant/mangrove>.
- Thom, B.G. (1982) 'Mangrove ecology: A geomorphological perspective. In, Mangrove Ecosystems in Australia, Structure, Function and Management (ed. B. Cluogh)', A.N.U. Press, Canberra, 3–17.
- Tomašík, J., Mokroš, M., Surový, P., Grznárová, A. and Merganič, J. (2019) 'UAV RTK/PPK Method—An Optimal Solution for Mapping Inaccessible Forested Areas?', *Remote sensing*, 11(6), 721. <https://doi.org/10.3390/rs11060721>.
- Tonkin, T.N. and Midgley, N.G. (2016) 'Ground-control networks for image based surface reconstruction: An investigation of optimum survey designs using UAV derived imagery and structure-from-motion photogrammetry', *Remote Sensing*, 8(9), 786. <https://doi.org/10.3390/rs8090786>.
- Topke, Katrien (2019) 'Mangroves', Available from <http://www.coastalwiki.org/wiki/Mangroves> [accessed on 15-07-2020].
- Torr, P. H. and Zisserman, A. (2000) 'MLE-SAC: A new robust estimator with application to estimating image geometry', *Computer vision and image understanding*, 78(1), 138-156. <http://dx.doi.org/10.1006/cviu.1999.0832>.
- Tsach, S., Tatievsky, A. and London, L. (2010) 'Unmanned Aerial Vehicles (UAVs)', *Encyclopedia of Aerospace Engineering*.
- Tsai, M.L., Chiang, K.W., Huang, Y.W., Lin, Y.S., Tsai, J.S., Lo, C.F., Lin, Y.S. and Wu, C.H. (2010) 'The development of a direct georeferencing ready UAV based photogrammetry platform', In *Proceedings of the 2010 Canadian Geomatics Conference and Symposium of Commission I*.
- Tuffen, H., James, M. R., Castro, J. M. and Schipper, C. I. (2013) 'Exceptional mobility of an advancing rhyolitic obsidian flow at Cordón Caulle volcano in Chile', *Nature communications*, 4(1), 1-7. <https://doi.org/10.1038/ncomms3709>.
- Turner, I.L., Harley, M.D. and Drummond, C.D. (2016) 'UAVs for coastal surveying', *Coastal Engineering*, 114, 19-24. <http://dx.doi.org/10.1016/j.coastaleng.2016.03.011>.

- Turner, D., Lucieer, A. and de Jong, S., (2015) 'Time Series Analysis of Landslide Dynamics Using an Unmanned Aerial Vehicle (UAV)', *Remote Sensing*, 7, 1736–1757. <https://doi.org/10.3390/rs70201736>.
- Turner, D., Lucieer, A. and Watson, C. (2012) 'An automated technique for generating georectified mosaics from ultra-high resolution unmanned aerial vehicle (UAV) imagery, based on structure from motion (SfM) point clouds', *Remote sensing*, 4(5), 1392-1410. <https://doi.org/10.3390/rs4051392>.
- Ullman, S. (1979) 'The interpretation of visual motion. MIT Press Series in Artificial Intelligence', MIT Press, Cambridge, Massachusetts, and London, England.
- Uysal, M., Toprak, A. S. and Polat, N. (2015) 'DEM generation with UAV Photogrammetry and accuracy analysis in Sahitler hill', *Measurement*, 73, 539-543. <http://dx.doi.org/10.1016/j.measurement.2015.06.010>.
- Valiela, I., J.L.Bowen and J.K. York, (2001) 'Mangrove forests: one of the worlds threatened major tropical environments', *BioScience*, 51(10), 807-815. [http://dx.doi.org/10.1641/0006-3568\(2001\)051\[0807:MFOOTW\]2.0.CO;2](http://dx.doi.org/10.1641/0006-3568(2001)051[0807:MFOOTW]2.0.CO;2).
- Vasuki, Y., Holden, E. J., Kovesi, P. and Micklethwaite, S. (2014) 'Semi-automatic mapping of geological Structures using UAV-based photogrammetric data: An image analysis approach', *Computers and Geosciences*, 69, 22-32. <http://dx.doi.org/10.1016/j.cageo.2014.04.012>.
- Villanueva, J.K.S. and Blanco, A.C. (2019) 'Optimization of ground control point (GCP) configuration for unmanned aerial vehicle (UAV) survey using structure from motion (SfM)', *International Archives of Photogrammetry Remote Sensing and Spatial Information Sciences*, 42, 167-174.
- Vosselman, G. (2000) 'Slope based filtering of laser altimetry data'. *International Archive of Photogrammetry and Remote Sensing*, 935-942.
- Wack, R. and Wimmer, A. (2002) 'Digital terrain models from airborne laser scanner data – a grid based approach', *International Archives of Photogrammetry Remote Sensing and Spatial Information Sciences*, 34, 293–296.
- Wang, Q., Wu, L., Xu, Z., Tang, H., Wang, R. and Li, F. (2014b) 'A progressive morphological filter for point cloud extracted from UAV images', *Geoscience and Remote Sensing Symposium, 2014 IEEE international*. 2014, 2023-2026.
- Wang, Y., Chen, H. and Li, H. (2018) '3D path planning approach based on gravitational search algorithm for sprayer UAV', *Transactions of the Chinese*

- Society for Agricultural Machinery*, 49(2), 28-33.
<http://dx.doi.org/10.6041/j.issn.1000-1298.2018.02.004>.
- Wang, R., Zhang, S., Pu, L., Yang, J., Yang, C., Chen, J., Guan, C., Wang, Q., Chen, D., Fu, B. and Sang, X. (2016) 'Gully erosion mapping and monitoring at multiple scales based on multi-source remote sensing data of the Sancha River Catchment, Northeast China', *ISPRS International Journal of Geo-Information*, 5(11), 200. <https://doi.org/10.3390/ijgi5110200>.
- Wang, L., Jia, M., Yin, D. and Tian, J. (2019) 'A review of remote sensing for mangrove forests: 1956–2018', *Remote Sensing of Environment*, 231, 111223. <https://doi.org/10.1016/j.rse.2019.111223>.
- Wei, W., Chen, D., Wang, L., Daryanto, S., Chen, L., Yu, Y., Lu, Y., Sun, G., and Feng, T. (2016) 'Global synthesis of the classifications, distributions, benefits and issues of terracing', *Earth-Science Review*. 159, 388–403. <http://dx.doi.org/10.1016/j.earscirev.2016.06.010>.
- Wells, J.T. and Roberts, H.H. (1980) 'Fluid mud dynamics and shoreline stabilization: Louisiana chenier plain', In: *Proceedings of the 17th International Conference on Coastal Engineering (Sydney)*. Part II: Coastal Sediment Problems, Chapter 84, pp. 1382-1401. American Society of Civil Engineers, New York.
- Wei, L., Yang, B., Jiang, J., Cao, G. and Wu, M. (2017) 'Vegetation filtering algorithm for UAV-borne lidar point clouds: a case study in the middle-lower Yangtze River riparian zone', *International Journal of Remote Sensing*, 38(8-10), 2991-3002. <https://doi.org/10.1080/01431161.2016.1252476>.
- Westaway, R. M., Lane, S. N. and Hicks, D. M. (2003) 'Remote survey of large-scale braided, gravel-bed rivers using digital photogrammetry and image analysis', *International Journal of Remote Sensing*, 24(4), 795-815. <https://doi.org/10.1080/01431160110113070>.
- Westoby, M. J., Brasington, J., Glasser, N. F., Hambrey, M. J. and Reynolds, J. M. (2012) 'Structure-from-Motion' photogrammetry: A low-cost, effective tool for geoscience applications', *Geomorphology*, 179, 300-314. <https://doi.org/10.1016/j.geomorph.2012.08.021>.
- Westoby, M., Brasington, J., Glasser, N., Hambrey, M., Reynolds, J., Hassan, M. and Lowe, A. (2015) 'Numerical modelling of glacial lake outburst floods using physically based dam-breach models', *Earth Surface Dynamics*, 3(1), 171-199. <http://dx.doi.org/10.5194/esurfd-2-477-2014>.

- Whitman, D., Zhang, K. (2005) 'Comparison of three algorithms for filtering airborne LiDAR data', *Photogrammetric Engineering and Remote Sensing*, 71 (3), 313–324. <http://dx.doi.org/10.14358/PERS.71.3.313>.
- Wheaton J.M. (2008) 'Uncertainty in Morphological Sediment Budgeting of Rivers', (PhD Thesis, University of Southampton).
- Wheaton, J.M., Brasington, J., Darby, S.E., Kasprak, A., Sear, D. and Vericat, D. (2013) 'Morphodynamic signatures of braiding mechanisms as expressed through change in sediment storage in a gravel-bed river', *Journal of Geophysical Research: Earth Surface*, 118(2), 759–779. <http://dx.doi.org/10.1002/jgrf.20060>.
- Wheaton, J., Brasington, J., Darby, S. and Sear, D. (2010) 'Accounting for uncertainty in DEMs from repeat topographic surveys: improved sediment budgets', *Earth Surface Processes and Landforms*, 35, 136–156. <http://dx.doi.org/10.1002/esp.1886>.
- Winterwerp, J.C., Borst, W.G. and de Vries, M.B. (2005) 'Pilot study on the erosion and rehabilitation of a mangrove mud coast', *Journal of Coastal Research* 21(2), 223–230. <http://dx.doi.org/10.2112/03-832A.1>.
- Williams, R. (2012) 'DEMs of Difference', *Geomorphological Techniques*, 2(3.2), 1–17.
- Williams, R. D, Brasington, J., Vericat, D., Hicks, D.M., Labrosse, F. and Neal. M. (2011) 'Monitoring braided river change using terrestrial laser scanning and optical bathymetric mapping'. In *Geomorphological mapping: methods and applications*, Smith M, Paron P, Griffiths J (eds). Elsevier: Amsterdam, 507–532.
- Wolanski, E. (1986) 'An evaporation-driven salinity maximum zone in Australian tropical estuaries', *Estuarine, Coastal and Shelf Science*, 22, 415–424. <https://doi.org/10.1016/0272-7714%2886%2990065-X>.
- Wolanski, E. (1989) 'Measurements and modeling of the water circulation in mangrove swamps', COMARF regional project for research and training on coastal marine systems in Africa- RAF/87/038. Serie Documentaire No. 3, 1–43.
- Wolanski, E. (1992) 'Hydrodynamics of mangrove swamps and their coastal waters' *Hydrobiologia*, 247, 141–161. <https://doi.org/10.1007/BF00008214>.

- Wolanski, E. (1995) 'Transport of sediment in mangrove swamps', *Hydrobiologia*, 295, 31-42. <https://doi.org/10.1007/BF00029108>.
- Wolanski, E. (2006) 'The application of ecohydrology for sustainable development and management of mangrovedominated estuaries', *The ICEMAN 2006 Mangrove Conference in Kuala Lumpur*.
- Wolanski, E., Jones, M. and Bunt, J.S. (1980) 'Hydrodynamics of a tidal creek-mangrove swamp system' *Australian Journal of Marine and Freshwater Research*, 31, 431-450. <https://doi.org/10.1071/MF9800431>.
- Woodroffe, C.D. (1992) 'Mangrove sediments and geomorphology', In, *Tropical Mangrove Ecosystems*. Coastal and Estuarine Studies 41 (eds. A.I. Robertson and D.M. Alongi), American Geophysical Union, Washington, D.C., 7-42.
- Woodroffe, C.D. and Davies, G. (2009) 'The morphology and development of tropical coastal wetlands'. In: *Coastal wetlands: An integrated ecosystem approach* (eds. Perillo, G., Wolanski, E., Cahoon, D. and Brinson, M.). 65-88. Elsevier.
- World Wildlife Fund (WWF) (2020) 'Mangrove Forest', Retrieved from https://www.wwf.org.my/about_wwf/what_we_do/forests_main/the_malaysian_rainforest/types_of_forests/mangrove_forests/.
- Xiaoqin, W., Miaomiao, W., Shaoqiang, W. and Yundong, W. (2015) 'Extraction of vegetation information from visible unmanned aerial vehicle images', *Transactions of the Chinese Society of Agricultural Engineering*, 31(5), 152-159. <http://dx.doi.org/10.3969/j.issn.1002-6819.2015.05.022>.
- Xiongkui, H., Bonds, J., Herbst, A. and Langenakens, J. (2017) 'Recent development of unmanned aerial vehicle for plant protection in East Asia', *International Journal of Agricultural and Biological Engineering*, 10(3), 18-30. <http://dx.doi.org/10.3965/j.ijabe.20171003.3248>.
- Young, B.M. and Harvey, L.E. (1996) 'A spatial analysis of the relationship between mangrove (*Avicennia marina* var. *australasica*) physiognomy and sediment accretion in the Hauraki Plains, New Zealand', *Estuarine, Coastal and Shelf Science*, 42, 231-246. https://ui.adsabs.harvard.edu/link_gateway/1996ECSS...42..231Y/doi:10.1006/ecss.1996.0017.
- Yilmaz, C.S. and Gungor, O. (2018) 'Comparison of the performances of ground filtering algorithms and DTM generation from a UAV-based point

- cloud', *Geocarto International*, 33(5), 522-537.
<https://doi.org/10.1080/10106049.2016.1265599>.
- Yilmaz, C.S., and Gungor, O., (2016) 'Comparison of the performances of ground filtering algorithms and DTM generation from a UAV-based point cloud', *Geocarto International*, 33(5), 522-537.
<http://dx.doi.org/10.1080/10106049.2016.1265599>.
- Yue, L., Shen, H., Zhang, L., Zheng, X., Zhang, F. and Yuan, Q. (2017) 'High-quality seamless DEM generation blending SRTM-1, ASTER GDEM v2 and ICESat/GLAS observations', *ISPRS Journal of Photogrammetry and Remote Sensing*, 123, 20-34. <http://dx.doi.org/10.1016/j.isprsjprs.2016.11.002>.
- Yun, B.Y. and Yoon, W.S. (2018) 'A Study on the Improvement of Orthophoto Accuracy According to the Flight Photographing Technique and GCP Location Distance in Orthophoto Generation Using UAV', *Journal of the Korean Society of Industry Convergence*, 21(6), 345-354.
<https://doi.org/10.21289/KSIC.2018.21.6.345>.
- Zeybek, M. and Şanlıoğlu, İ. (2019) 'Point cloud filtering on UAV based point cloud', *Measurement*, 133, 99-111.
<https://doi.org/10.1016/j.measurement.2018.10.013>.
- Zhang, H., Aldana-Jague, E., Clapuyt, F., Wilken, F., Vanacker, V. and Van Oost, K. (2019) 'Evaluating the potential of post-processing kinematic (PPK) georeferencing for UAV-based structure-from-motion (SfM) photogrammetry and surface change detection', *Earth Surface Dynamics*, 7(3), 807-827.
<https://doi.org/10.5194/esurf-7-807-2019>.
- Zhang, W., Qi, J., Wan, P., Wang, H., Xie, D., Wang, X., and Yan, G. (2016) 'An easy-to-use airborne LiDAR data filtering method based on cloth simulation', *Remote Sensing* 8 (6), 501. <https://doi.org/10.3390/rs8060501>.
- Zhang, K., Chen, S.-C., Whitman, D., Shyu, M.-L., Yan, J., Zhang, and C., (2003) 'A progressive morphological filter for removing nonground measurements from airborne LIDAR data', *IEEE Transaction of Geoscience and Remote Sensing*, 41, 872-882. <https://doi.org/10.1109/TGRS.2003.810682>.
- Zhang, K., Liu, H., Li, Y., Xu, H., Shen, J., Rhome, J. and Smith, T.J. (2012) 'The role of mangroves in attenuating storm surges', *Estuarine, Coastal and Shelf Science*, 102, 11-23. <http://dx.doi.org/10.1016/j.ecss.2012.02.021>.

- Zimmer, B., Liutkus-Pierce, C., Marshall, S.T., Hatala, K.G., Metallo, A. and Rossi, V. (2018) 'Using differential structure-from-motion photogrammetry to quantify erosion at the Engare Sero footprint site, Tanzania', *Quaternary Science Reviews*, 198, 226–241.
<https://doi.org/10.1016/j.quascirev.2018.07.006>.
- Zongjian, L.I.N. (2008) 'UAV for mapping—low altitude photogrammetric survey'. *International Archives of Photogrammetry and Remote Sensing, Beijing, China*, 37, 1183-1186.

LIST OF PUBLICATIONS

Journal with Impact Factor

- 1 **Mohamad, N.**, Ahmad, A., Khanan, M.F.A., and Din, A.H.M. (2022). Surface Elevation Changes Estimation underneath Mangrove Canopy Using SNERL Filtering Algorithm and DoD Technique on UAV-Derived DSM Data. *ISPRS International Journal of Geo-Information*, 11(1), 32. <http://dx.doi.org/10.3390/ijgi11010032> (**Q2, IF: 3.099**).
- 2 Khalid, N.F., Din, A.H.M., Khanan, M.F.A., **Mohamad, N.**, Hamid, A.I.A., and Ahmad, A. (2021). Potential vulnerability impact of coastal inundation over Kelantan coast due to sea level rise based on satellite altimetry, GPS and LiDAR data. *Arabian Journal of Geoscience*, 14. <https://doi.org/10.1007/s12517-021-08539-5>. (**Q3, IF: 1.827**).
- 3 **Mohamad, N.**, Abdul Khanan, M. F., Ahmad, A., Md Din, A. H., and Shahabi, H. (2019). Evaluating water level changes at different tidal phases using UAV photogrammetry and GNSS vertical data. *Sensors*, 19(17), 3778. <http://dx.doi.org/10.3390/s19173778>. (**Q1, IF: 3.847**).

Indexed Journal

- 1 **Mohamad, N.**, Ahmad, A., Khanan, M.F.A., and Din, A.H.M. (2021). Utilising Multi-Temporal VHR Satellite Imageries for Erosion and Accretion Assessment at Mangrove Ecosystem. **Submitted** in *International Journal of Integrated Engineering*, Penerbit UTHM, Malaysia. (**Indexed by SCOPUS and WOS**).

- 2 **Mohamad, N.**, Ahmad, A., and Din, A.H.M. (2021). Estimation of Surface Elevation Changes at Bare Earth Riverbank using Differential DEM Technique of UAV Imagery Data. *Geografia-Malaysian Journal of Society and Space*, 17 (4). <https://doi.org/10.17576/geo-2021-1704-23>. **(Indexed by WOS)**.
- 3 **Mohamad, N.**, Ahmad, A., and Din, A.H.M. (2021). A Review of UAV Photogrammetry Application in Assessing Surface Elevation Changes. **Accepted** in *Journal of Information System and Technology Management (JISTM)*, 7(25). <https://doi.org/10.35631/JISTM.725016>. **(Indexed by MyCite)**.

Indexed Conference Proceeding

- 1 **Mohamad, N.**, Khanan, M.F.A., Ahmad, A., and Din, A.H.M. (2020). Derivation of MSL Riverbank Line from UAV DSM Data based on Tidal Slope Analysis. In *7th International Conference on Geomatics and Geospatial Technology (GGT 2021)*, 767 (2021) 012017. IOP Conference Series: Earth and Environmental Science. <http://dx.doi.org/10.1088/1755-1315/767/1/012017>. **(Indexed by SCOPUS)**.
- 2 **Mohamad, N.**, Ahmad, A. and Din, A.H.M. (2020). Monitoring Groundwater Depletion Due to Drought using Satellite Gravimetry: A Review. In *10th IGRSM International Conference and Exhibition on Geospatial and Remote Sensing (IGRSM 2020)*, 540 (2020) 012054. IOP Conference Series: Earth and Environmental Science. <http://dx.doi.org/10.1088/1755-1315/540/1/012054>. **(Indexed by SCOPUS)**.

Non-Indexed Conference Proceeding

- 1 **Mohamad, N.**, Khanan, M.F.A., Ahmad, A., and Din, A.H.M. (2020). Forecasting Future Riverbank Erosion Model Using Kernel Density and Line Buffering Method. In *8th International Graduate Conference On Engineering, Science and Humanities (IGCESH 2020)* Abstract Proceeding, Universiti Teknologi Malaysia, Johor, Malaysia.

Book Chapter

- 1 Razak, M. Z. A., Din, A.H.M, Zulkifli, N. A, and **Mohamad, N.** (2021). Estimating Groundwater Storage in Peninsular Malaysia from GRACE Satellite Data. **Under Review** in *UTM Press, Universiti Teknologi Malaysia*.